NASA Technical Memorandum 107574

HIERARCHICAL FLUX-BASED THERMAL-STRUCTURAL FINITE ELEMENT ANALYSIS METHOD

Sandra P. Polesky

April 1992

National Aeronautics and
Space Administration

Langley Research Center
Hampton, Virginia 23665

HIERARCHICAL FLUX-BASED THERMAL-STRUCTURAL FINITE ELEMENT ANALYSIS METHOD

by
Sandra P. Polesky

ABSTRACT

A hierarchical flux-based finite element method is developed for both one- and two-dimensional thermal-structural analyses. Derivation of the finite element equations is presented. The resulting finite element matrices associated with the flux-based formulation are evaluated in closed-form. The hierarchical finite elements include additional degrees of freedom in the approximation of the element variable distributions by the use of nodeless variables. The nodeless variables offer increased solution accuracy without the need for defining actual nodes and rediscretizing the finite element model. Thermal and structural responses obtained using the hierarchical flux-based method are compared with results obtained from a conventional linear finite element method and exact solutions. Results show that the hierarchical flux-based method can provide improved thermal and structural solution accuracy with fewer elements when compared to results for the conventional linear element method.

TABLE OF CONTENTS

LIST OF FIGURES iv

LIST OF SYMBOLS v

Chapter

1 INTRODUCTION 1

1.1 Overview 1

1.2 Literature Review 2

1.3 Objective 4

2 FLUX-BASED FINITE ELEMENT FORMULATION 6

2.1 Basic Concepts 6

2.2 Governing Equations 7

2.2.1 Thermal Analysis 7

2.2.2 Structural Analysis 8

2.3 Solution Procedure 9

2.4 Closed-Form Finite Element Matrices 15

3 ONE-DIMENSIONAL NODELESS VARIABLE FINITE ELEMENTS USING FLUX-BASED FORMULATION 19

3.1 Element Interpolation Functions 19

3.2 Derivation of Flux-based Finite Element Equations 22

3.2.1 Thermal Analysis 22

3.2.2 Structural Analysis 27

3.3 Thermal-Structural Analysis Algorithm 31

3.4 Applications of One-Dimensional Methodologies 33

3.4.1 Transient Thermal Analysis of a Copper Slab 34

3.4.2 Thermal-Structural Analysis of a Copper Rod 38

4 TWO-DIMENSIONAL NODELESS VARIABLE FINITE ELEMENTS USING FLUX-BASED FORMULATION 46

4.1 Element Interpolation Functions 46

4.2 Derivation of Flux-based Finite Element Equations 50

4.2.1 Thermal Analysis 50

4.2.2 Structural Analysis 55

4.3 Applications of Two-Dimensional Methodologies 62

5 CONCLUDING REMARKS 71

REFERENCES..... 73

Appendices

A Closed-Form Matrices for One-Dimensional Nodeless Variable Flux-based Finite Element..... 77

B Closed-Form Matrices for Two-Dimensional Nodeless Variable Flux-based Finite Element..... 79

LIST OF FIGURES

Figure — Page

1. Four-node quadrilateral finite element in Cartesian and natural coordinates 11
2. One-dimensional thermal finite element and typical element temperature distributions 20
3. Flow chart for one-dimensional hierarchical flux-based thermal-structural analysis 32
4. Schematic diagram of thermal finite element model of a copper slab and material properties for copper 35
5. Case one: Temperature distributions in a copper slab with constant material properties 37
6. Case two: Temperature distributions in a copper slab with temperature dependent conductivity at t = 0.0001 sec 39
7. Schematic diagrams of thermal and structural finite element models of a copper rod 40
8. Temperature distributions in a copper rod at t = 0.5 sec 41
9. Case one: Displacement distributions in a copper rod subjected to thermal loading and constrained at x = 0 43
10. Case two: Structural response for a copper rod with both ends constrained 44
11. Typical two-dimensional finite element temperature distributions 49
12. Schematic diagram of structural finite element model and assumed temperature distribution 64
13. Displacement distributions in a copper plate subjected to a linear temperature distribution 65
14. Schematic diagram of thermal and structural finite element model of a copper plate 67
15. Temperature distributions in a copper plate at t = 5 sec 68
16. Displacement and stress distributions in a copper plate at t = 5 sec 72

LIST OF SYMBOLS

A	element area
c	specific heat
[C]	matrix of material elastic constants
$[C_p]$	capacitance matrix
[B]	boundary matrix
$[B_s]$	interpolation function gradient matrix
[D]	internal matrix
E, F	heat flux or stress components in the x- and y-coordinate directions, respectively
H	heat load
h	convective heat transfer coefficient
k	thermal conductivity
[K]	conductivity matrix
L	element length
[LHS]	left hand side matrix
[M]	mass matrix
N	no
N_i	element interpolation functions
{N}	vector of element interpolation functions
[N]	combined matrix for structural interpolation functions
[P]	matrix relating first stress component to displacement
q	aerodynamic heating
q_x, q_y	components of heat conduction in x- and y-coordinate directions, respectively
{RHS}	right hand side vector

$\{R\}$	load vector
T	temperature
$\{T\}$	nodal temperature vector
$\{T_s\}$	surface traction vector
T_o	reference temperature for zero thermal stress
T_r	fluid recovery temperature
T_∞	surrounding medium temperature
t	time
U	variable in heat transfer equation
u	element displacement distribution in x-coordinate direction
$\{u\}$	nodal displacement vector for x-coordinate direction
v	element displacement distribution in y-coordinate direction
$\{v\}$	nodal displacement vector for y-coordinate direction
x, y	Cartesian coordinate directions
$\{x\}$	element nodal coordinates in x-direction
$\{y\}$	element nodal coordinated in y-direction
Y	yes
ζ, η	natural coordinate directions
ρ	material density
Δt	time step
ΔU	change in variable U per time step
ΔT	change in temperature per time step
β	thermal expansion parameter
δ	combined displacement vector
ε	emissivity
ε_i	strain components
E	modulus of elasticity

σ	Stefan-Boltzmann constant or element stress
σ_1	first stress component
σ_2	second stress component
σ_x, σ_y, τ_{xy}	components of stress tensor
ν	Poisson's ratio
α	coefficient of thermal expansion

Subscripts

i	nodal number reference
n	normal
S	structural component
T	thermal component
x, y	Cartesian coordinate directions
1	first component
2	second component

Superscripts

T	transpose
n	time step index, $t^n = n\Delta t$

Chapter 1
INTRODUCTION

1.1 Overview

The finite element method provides a valuable technique for structural analysis and design. The method is well suited for the analysis of structures with various geometries, loadings, and boundary conditions. Although other computational techniques are available, the finite element method is usually best suited for problems having complex geometries. A thorough evaluation of the structural response induced by aerodynamic loading is an important factor in the design of aircraft structures. Thermal and structural finite element analyses are often required in the design of high-speed aerospace vehicles to prevent structural failure and enhance structural performance.

For high-speed aircraft, severe aerodynamic heating may occur in local areas on the body of the vehicle. Nonuniform heating may produce intense local thermal gradients. Since thermal stresses are sensitive to thermal gradients, a detailed thermal analysis is required to predict accurate temperature distributions needed for evaluation of the thermal stresses. The finite element model generally needs to be discretized several times to assure convergence and accuracy of the thermal and structural solutions. The process of discretizing the finite element model can be time consuming for complicated

structures and can result in an increasing number of degrees of freedom which increases the computational expense. An additional time consuming process can be incurred in the transfer of data from the thermal analysis to a form suitable for input into the structural analysis. Since the finite element method is a widely accepted analysis technique, difficulties and inadequacies in applying the method have inspired research for improving the accuracy and efficiency of the method.

1.2 Literature Review

The finite element method was first introduced in 1956 as a means for analyzing complex aircraft structures [1]. Since its inception, the finite element method has become one of the most prominent numerical methods for structural analysis. More recently, the finite element method has gained wider acceptance for the analysis of thermal and fluid problems. The conventional formulation of the finite element equations in all three disciplines and the most commonly used element interpolation functions for defining the element distribution of the unknown dependant variables can be found in reference 2.

In general, the accuracy of the finite element solution is improved by refining the finite element model using consecutively smaller elements until there is convergence of the solution. The method for improving solution accuracy by decreasing the element size is known as the h-method. A commonly used alternative approach, the p-method, redefines the element interpolation functions using more nodes with higher-order interpolation functions until the solution converges. An integrated thermal-structural finite element approach was introduced by Dechaumphai and Thornton [3-5] which improves the solution accuracy and computational efficiency for predicting

thermal stresses. The integrated thermal-structural finite element method uses a nodeless variable formulation, where additional unknown variables are included in the assumed element distribution. These nodeless variables are associated with quadratic interpolation functions which produce more accurate solutions than the conventional linear element formulation. The nodeless variable formulation provides more accurate transient temperature distributions by increasing the degrees of freedom of the element without defining additional element nodes, and consequently may yield more accurate thermal stress predictions without the need for rediscretizing the finite element model. The use of nodeless variables can also be referred to as a hierarchical methodology, since the formulation reduces to the conventional linear element formulation when the nodeless variables are constrained to zero or eliminated.

Other approaches for improving the finite element method include the development of efficient algorithms for generating the finite element equations. A Taylor-Galerkin algorithm, first developed by Donea [6-7] for convective transport problems, was applied for the analysis of high-speed flows [8-11]. The desire for a single methodology to analyze combined fluid, thermal, and structural interactions led to the extension of the Taylor-Galerkin algorithm for the thermal and structural finite element formulations [12-13]. An integrated fluid-thermal-structural analysis method [14] was developed for the two-dimensional analysis of high-speed flow over leading edges of aerospace vehicles. A key feature of the Taylor-Galerkin algorithm is the use of the flux-based formulation, where the distribution of the flux of the dependent variable is assumed in the same form as the distribution of the dependant variable. The flux-based formulation leads to finite element matrices that can be evaluated in closed form, whereas the conventional finite element formulation requires numerical integration. Another benefit of the algorithm is that nonlinear material

properties can be included directly and do not require regeneration of the finite element matrices. Also, nonlinear boundary conditions can be incorporated easily into the analysis algorithm. These benefits of the flux-based methodology led to the further extension of the algorithm for the three-dimensional thermal-structural analysis of high-speed wing leading edge designs [15-16]. Additionally, a standard two-dimensional eight-node higher-order element was incorporated with the flux-based finite element method for transient thermal analyses [17]. The use of such a higher-order element requires defining additional nodes within the element and consequently redefining the finite element model.

1.3 Objective

The objective of this thesis is to develop an improved finite element method for predicting accurate thermal and structural responses of structures. As an alternative to using higher-order elements, which requires redefining the finite element model with additional nodes, this thesis develops and investigates the use of nodeless variable finite elements with the flux-based finite element formulation. The hierarchical flux-based finite elements have the potential of offering a more efficient means of obtaining an accurate thermal-structural solution. Both the one- and two-dimensional hierarchical flux-based elements are developed for thermal and structural analyses. Transient thermal and quasi-static structural analysis capabilities have been developed and are contained in a common computer program. The thermal finite element model and its temperature solution are completely compatible with the structural finite element model. No transfer or manipulation of data is required to obtain the thermal loading used in the structural analysis. The finite element results are

compared with results obtained using EAL (Engineering Analysis Language [18]), a general purpose finite element code frequently used for the thermal and structural analyses of aircraft structures.

Details of the flux-based finite element method for thermal and structural analyses are presented in Chapter 2. The basic concepts are introduced along with the benefits of the algorithm as compared to the conventional finite element formulation. The concept of nodeless variable finite elements, which were developed in reference 3 using the conventional finite element formulation, is introduced in Chapter 3. Later in this chapter, a one-dimensional hierarchical thermal-structural flux-based finite element analysis method is developed and results of the method are presented. The methodology is extended to two-dimensional elements in Chapter 4 with the development of a membrane thermal-structural analysis capability. A summary of the results and concluding remarks concerning the effect on accuracy in using the hierarchical flux-based finite element method for thermal and structural analyses is presented in Chapter 5.

Chapter 2
FLUX-BASED FINITE ELEMENT FORMULATION

2.1 Basic Concepts

A common approach to the formulation of many thermal-structural problems is to assume that the thermal and structural analyses are uncoupled, and that the structural analysis is quasi-static. The thermal and structural analyses are uncoupled by neglecting the mechanical deformation rate that could alter the temperature in the heat transfer equation. In addition, by neglecting the inertia term in the structural equation of motion, the structural analysis is deemed quasi-static. These assumptions are credible when the temperature change is slow and the coupling effect is negligible. The assumptions allow the transient thermal analysis to be performed first, and the series of resulting temperatures are then used in performing the structural analysis. This approach was applied in the development of the Taylor-Galerkin algorithm with a flux-based formulation for thermal-structural analyses [12]. The flux-based formulation allows the finite element matrices to be evaluated in closed form, and distinguishes the method from the conventional formulation, where numerical integration is required. In addition, the flux-based formulation has desirable attributes that make it effective for analyzing large transient thermal-structural problems, where the thermal analysis can be nonlinear. First, the time required to form the finite element matrices using the closed form expressions is considerably less than the conventional method, which requires numerical integration [15]. Additionally, nonlinear effects, such as temperature

dependent material properties, are easily included in the analysis, and do not require regeneration of the finite element matrices as in the conventional formulation. Because these advantages improve computational efficiency over conventional methods, the flux-based algorithm is considered to be more suitable for solving complex problems. The development of the finite element formulation for transient thermal and quasi-static structural analysis using the flux-based formulation is presented in this chapter as a prelude to the extension of the flux-based formulation to nodeless variable elements in the following chapters. A comparison to the conventional method is made for the two-dimensional thermal analysis formulations to present the effect of the flux-based formulation on the finite element equations.

2.2 Governing Equations

2.2.1 Thermal Analysis

For an uncoupled thermal-structural analysis, the energy equation describing the transient thermal response of the structure in two dimensions can be written in the form,

$$\frac{\partial U_T}{\partial t} + \frac{\partial E_T}{\partial x} + \frac{\partial F_T}{\partial y} = H_T \tag{2.1}$$

where U_T is related to the internal energy, the subscript T denotes the thermal analysis, E_T and F_T are the heat transfer components in the x- and y-coordinate directions, respectively, and H_T is the internal heat generation. The variable U_T and the heat transfer components can be expressed in terms of the temperature as,

$$\frac{\partial U_T}{\partial t} = \rho\, c \frac{\partial T}{\partial t}$$

$$E_T = q_x = -k \frac{\partial T}{\partial x} \qquad (2.2)$$

$$F_T = q_y = -k \frac{\partial T}{\partial y}$$

where ρ is the density, c is the specific heat, k is the thermal conductivity, and T is the temperature. As shown in equation (2.2), the components of heat flux in the two coordinate directions (q_x and q_y) are assumed to be related to temperature gradients by Fourier's law. Both the specific heat and the thermal conductivity may be temperature dependent.

2.2.2 Structural Analysis

The quasi-static structural response is governed by the equilibrium equations that can be written in the form,

$$\frac{\partial \{E_S\}}{\partial x} + \frac{\partial \{F_S\}}{\partial y} = 0 \qquad (2.3)$$

where the subscript S denotes the structural analysis. For two-dimensional problems the vectors $\{E_S\}$ and $\{F_S\}$ contain the stress components given by

$$\{E_S\}^T = [\ \sigma_x \quad \tau_{xy}\ ]$$
$$\{F_S\}^T = [\ \tau_{xy} \quad \sigma_y\ ] \qquad (2.4)$$

where the stress components σ_x, σ_y, and τ_{xy} are assumed to be related to displacement gradients and the temperature by generalized Hooke's law,

$$\{\sigma\} = [C]\{\varepsilon\} + \{\beta\}(T-T_o) \tag{2.5}$$

where $\{\sigma\}$ is the vector of stress components, $\{\varepsilon\}$ is the vector of strain components, [C] is the matrix of material elastic constants, $\{\beta\}$ is the vector of thermal expansion parameters, T is the temperature, and T_o is the reference temperature for a zero stress state.

2.3 Solution Procedure

For simplicity and to illustrate the generality of the flux-based algorithm, the thermal or structural governing equation is written in the form of a single equation as

$$\frac{\partial U}{\partial t} + \frac{\partial E}{\partial x} + \frac{\partial F}{\partial y} = 0 \tag{2.6}$$

where the first term is zero for the quasi-static structural formulation.

The basic objectives of the Taylor-Galerkin algorithm are to: (1) use a Taylor series expansion of the U variable to establish recursion relations, and (2) use the Galerkin method of weighted residuals [2] for spatial discretization to derive the finite element equations. A more detailed description of the Taylor-Galerkin algorithm is presented in the following chapters for the development of the nodeless variable flux-based finite element equations.

For the thermal analysis formulation, the temperature, T, is the dependent variable and is contained in U, where

$$\frac{\partial U}{\partial t} \cong \frac{\Delta U}{\Delta t} = \rho c \frac{\Delta T}{\Delta t} \tag{2.7}$$

The term ΔT is the change in temperature from the previous time step, n, to the current time step, n+1, where $\Delta T = (T^{n+1} - T^n)$. The next step in the formulation of the finite element equations is to assume a spatial variation of the dependent variable throughout the selected element type. A natural coordinate system, which simplifies the element geometry, is used to define the spatial variations in non-dimensional form. The distribution of temperature, T, for the four-node bilinear quadrilateral element, is assumed in the form

$$T(x,y,t) = \sum_{i=1}^{4} N_i(\zeta,\eta)\, T_i(t) = \{N(\zeta,\eta)\}^T \{T(t)\} \tag{2.8}$$

where $\{N(\zeta,\eta)\}^T$ is the row matrix of the nodal interpolation functions in natural coordinates, ζ and η, and $\{T\}$ is the vector of nodal temperatures. A conventional four-node quadrilateral element shape is shown in figure 1(a) and the transformation to the natural coordinates is shown in figure 1(b). Since finite element matrices are in the form of integrals over element areas, transformation to natural coordinates permits the integrals to be evaluated over a square region. The Cartesian coordinates are related to the natural coordinates by

$$\begin{aligned} x &= [N(\zeta,\eta)]\,\{x\} \\ y &= [N(\zeta,\eta)]\,\{y\} \end{aligned} \tag{2.9}$$

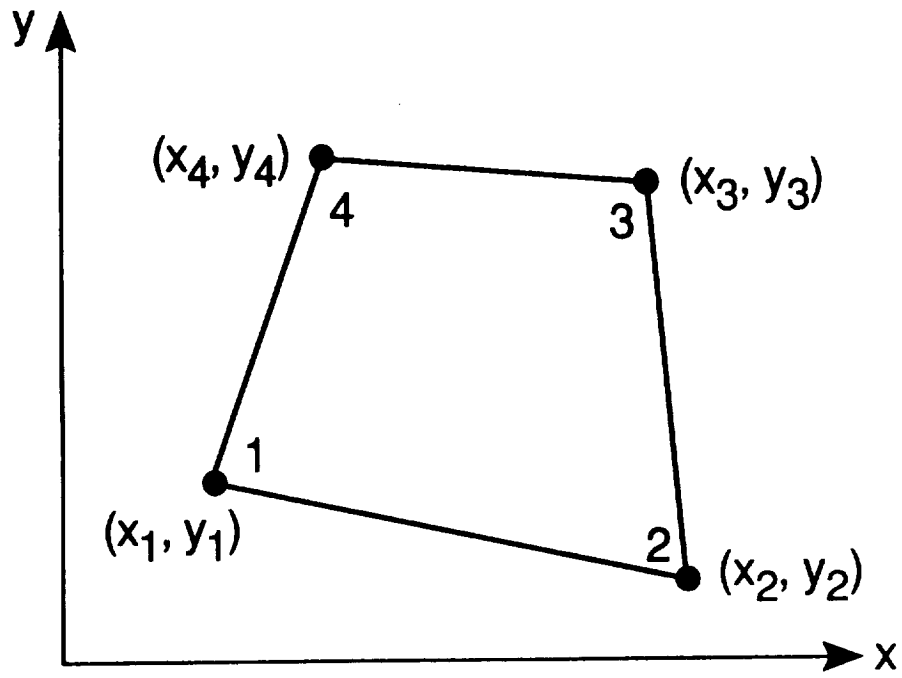

(a) Cartesian coordinates

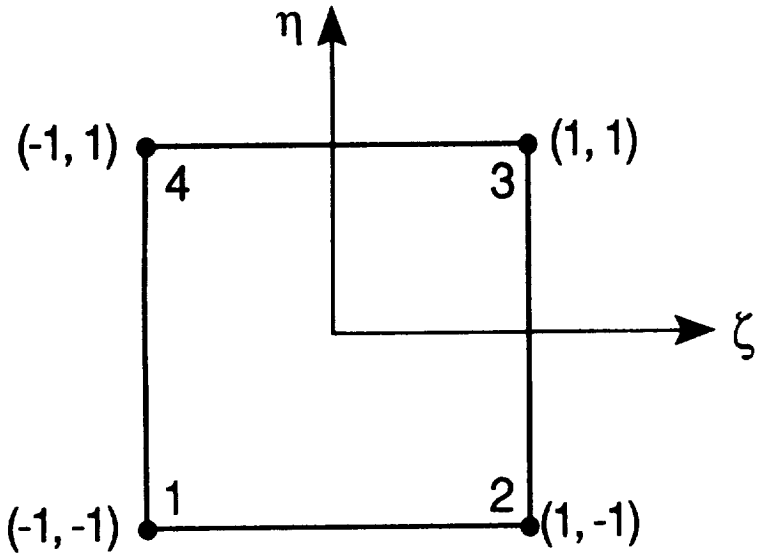

(b) Natural coordinates

Figure 1. Four-node quadrilateral finite element in Cartesian and natural coordinates.

where {x} and {y} are the vectors of nodal Cartesian coordinates for the element. Since the same interpolation functions, N_i, are used to interpolate the temperature and the spatial coordinates, the element is called an isoparametric element. For the four-node quadrilateral element, the interpolation functions are defined by

$$\begin{aligned} N_1 &= \frac{1}{4}(1-\zeta)(1-\eta) \\ N_2 &= \frac{1}{4}(1+\zeta)(1-\eta) \\ N_3 &= \frac{1}{4}(1+\zeta)(1+\eta) \\ N_4 &= \frac{1}{4}(1-\zeta)(1+\eta) \end{aligned} \tag{2.10}$$

The variable, U, which is directly related to T, is also assumed in the same form as equation (2.8). As a consequence of the Taylor-Galerkin algorithm, U becomes the unknown variable. The thermal finite element equations are solved for U at each time step. The temperatures are then determined from equation (2.7).

A feature of the flux-based algorithm, which differs from the conventional finite element method, is that the flux-based algorithm expresses the variation of the element fluxes E and F in the same form as the element dependent variable [6-7], that is

$$\begin{aligned} U(x,y,t) &= [N(\zeta,\eta)]\{U(t)\} \\ E(x,y,t) &= [N(\zeta,\eta)]\{E(t)\} \\ F(x,y,t) &= [N(\zeta,\eta)]\{F(t)\} \end{aligned} \tag{2.11}$$

where {U} is the vector of unknown nodal quantities of the variable U. In the thermal context, {E} and {F} are the vectors of the element nodal heat fluxes and are related to the nodal temperatures by equation (2.2) and equation (2.7). In the structural context, {E} and {F} are vectors of the element nodal stresses, which are related to the unknown nodal displacements by use of equation (2.5) and the strain-displacement relations.

Application of the Taylor-Galerkin algorithm to the energy equation, equation (2.1), and the flux-based assumption [12] results in the transient thermal finite element equation

$$[M]\{\Delta U\}^n = \{R_x\}_1^n + \{R_y\}_1^n + \{R\}_2^n \tag{2.12}$$

where [M] denotes the mass matrix

$$[M] = \int_A \{N\}\{N\}^T dA \tag{2.13}$$

which may be diagonalized to produce a lumped mass matrix. The vector $\{\Delta U\}^n$ is the change in the nodal values of the variable U between the time steps t^{n+1} and t^n where $t^n = n\Delta t$. The vectors $\{Rx\}_1^n$ and $\{Ry\}_1^n$ are associated with the fluxes within the element in the x- and y-coordinate directions and $\{R\}_2^n$ is the boundary term associated with the flux across the element boundary. These vectors are defined by

$$\{R_x\}_1^n = \Delta t\,[D_x]\,\{E\}^n \tag{2.14a}$$

where

$$[D_x] = \int_A \frac{\partial\{N\}}{\partial x} \{N\}^T dA \tag{2.14b}$$

$$\{R_y\}_1^n = \Delta t\, [D_y]\, \{F\}^n \tag{2.15a}$$

where

$$[D_y] = \int_A \frac{\partial\{N\}}{\partial y} \{N\}^T dA \tag{2.15b}$$

$$\{R\}_2^n = -\Delta t\, [B]\, \{q\} \tag{2.16a}$$

where

$$[B] = \int_S \{N\}\{N\}^T dS \tag{2.16b}$$

The vector {q} contains the components of the nodal heat flux normal to the element surface boundary. The thermal boundary conditions are applied with the vector {q} expressed in equation (2.16a), where the surface nodal heat flux q is replaced by the quantities representing any one of several different types of boundary conditions

$$q = \begin{cases} 0 & \text{(insulated)} \\ q_s & \text{(specified heating)} \\ h(T-T_r) & \text{(surface convection)} \\ \varepsilon\sigma(T^4-T_\infty^4) & \text{(surface radiation)} \end{cases} \tag{2.17}$$

For the structural analysis, the Taylor-Galerkin flux-based formulation produces matrices identical to equations (2.14-2.16), where {E} and {F} represent the nodal stress components given in equation (2.4). More details of the formulation and boundary conditions for the structural analysis are given in reference 15.

2.4 Closed-Form Finite Element Matrices

All the element integrals obtained from the flux-based formulation can be evaluated in closed form. The closed-form matrices apply to the quadrilateral as well as the hexahedral element shapes. The availability of closed-form expressions eliminates the need for numerical integration in the evaluation of element matrices. The closed-form expressions for the flux-based finite element matrices, [M], $[D_x]$, $[D_y]$, and [B] defined in equations (2.13-2.16), are merely a function of the element geometry. The use of the symbolic manipulation program, MACSYMA [19], simplified the evaluation of the closed-form expressions. The closed-form expressions for the coefficients in the finite element matrix $[D_x]$, for the four-node quadrilateral element are

$$
\begin{aligned}
D_x(1,1) &= -D_x(3,3) = -(y_4 - y_2)/6 \\
D_x(2,2) &= -D_x(4,4) = -(y_1 - y_3)/6 \\
D_x(1,3) &= -D_x(3,1) = -(y_4 - y_2)/12 \\
D_x(2,4) &= -D_x(4,2) = -(y_1 - y_3)/12 \\
D_x(1,2) &= -(y_4 + y_3 - 2y_2)/12 \\
D_x(1,4) &= -(2y_4 + y_3 - y_2)/12 \\
D_x(2,1) &= (y_4 + y_3 - 2y_1)/12 \\
D_x(2,3) &= -(y_4 - 2y_3 + y_1)/12
\end{aligned}
\qquad (2.18)
$$

$$D_x(3,2) = (y_4 - 2y_3 - y_1) / 12$$

$$D_x(3,4) = (2y_4 - y_2 - y_1) / 12$$

$$D_x(4,1) = -(y_3 + y_2 - 2y_1) / 12$$

$$D_x(4,3) = -(2y_3 - y_2 - y_1) / 12$$

where x_i and y_i are the nodal coordinates. Expressions for $[D_y]$, [M] and [B] are similar and are given in reference 15. The flux-based finite element matrices are also independent of material properties. This feature removes the necessity of reforming the element matrices at every time step when material properties are temperature dependent.

The formulation of the finite element equations using the conventional finite element method also begins with the governing equations for heat transfer and structural equilibrium expressed in equations (2.1- 2.4). For the thermal quadrilateral element formulation, the temperature is also assumed to be in the same form as equation (2.8) using the element interpolation functions defined in equation (2.10) and the natural coordinate transformation expressed in equation (2.9). The thermal finite element equations are in the form

$$[C_p] \{\frac{\partial T}{\partial t}\} + [K_x]\{T\} + [K_y] \{T\} = \{H\} \qquad (2.19)$$

where {T} is the vector of unknown nodal temperatures, $[C_p]$ is referred to as the capacitance matrix, {H} is the internal heat generation vector, and $[K_x]$ and $[K_y]$ are the conductance matrices associated with heat conduction in the x- and y-coordinate directions, respectively. The matrices are defined by

$$[C_p] = \int_A \rho c \{N\} \{N\}^T \, dA \qquad (2.20)$$

$$[K_x] = \int_A k \frac{\partial\{N\}}{\partial x} \frac{\partial\{N\}^T}{\partial x} dA \qquad (2.21)$$

$$[K_y] = \int_A k \frac{\partial\{N\}}{\partial y} \frac{\partial\{N\}^T}{\partial y} dA \qquad (2.22)$$

where ρ is the density, c is the specific heat and k is the thermal conductivity. It can be observed from equations (2.20-2.22) that the conventional finite element matrices are dependent on the material properties which, in general, are a function of the temperature. In addition, there is no closed-form expression for $[K_x]$ and $[K_y]$ for arbitrary quadrilateral element shapes. Numerical integration is thus required to compute these element matrices. The Gauss integration method is used where the integral is expressed as a sum of the weighted terms evaluated at Gauss points. Gauss weighting factors and integration points can be found in reference 2. In performing numerical integration, the accuracy of the matrices depends on the number of Gauss points used. Two Gauss points in each coordinate direction are normally used for the bilinear quadrilateral element. Due to their dependency on material properties and the need for numerical integration, the process of generating the conventional finite element matrices can be computationally expensive.

To predict temperatures and temperature gradients accurately in a structure subjected to aerodynamic heating, refined finite element mesh sizes may be needed at some locations. Finer meshes, and hence smaller elements, require small time steps for analysis solution stability, such as for explicit solution algorithms. Hence, the finite element equation needs to be solved many times when performing a transient thermal analysis. Temperature dependent material properties are also often necessary to model thermal effects accurately in a transient thermal analysis. These requirements may make the

conventional finite element method computationally expensive for modelling large-scale aircraft structures. The flux-based finite element method offers the advantages of closed-form finite element matrices and ease in representing temperature dependent material properties while providing equivalent solution accuracy. Hence, the flux-based finite element method may be more suitable for analyzing large nonlinear, transient thermal-structural problems. The benefits of the flux-based finite element method inspired the extension to nodeless variable elements developed herein.

Chapter 3

ONE-DIMENSIONAL NODELESS VARIABLE FINITE ELEMENTS USING FLUX-BASED FORMULATION

3.1 Element Interpolation Functions

The fundamental basis of the finite element method is that a continuum of arbitrary shape can be modeled by an assemblage of simple shapes. For one-dimensional problems, the elements are line segments. The line segments are assembled to model a one-dimensional domain, which may be either a one-dimensional slab or rod continuum. The variation of a dependent variable within the element is then approximated as a function of the nodal variables and interpolation functions. The conventional finite element method normally utilizes linear elements where a linear distribution of a dependent variable within an element is assumed using linear interpolation functions.

For hierarchical finite elements, additional unknown variables, sometimes called nodeless variables, are introduced in the assumed distribution of a dependent variable for an element to provide a nonlinear distribution of the dependent variable. For thermal problems, temperature is the dependent variable. A two-node one-dimensional element and typical element temperature distributions for the conventional and hierarchical finite elements are shown in figure 2. The hierarchical finite element with one nodeless variable assumes the element temperature distribution in the form

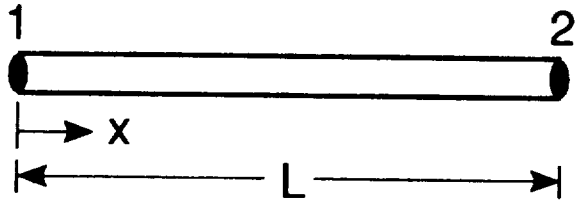

(a) Two-node one-dimensional element

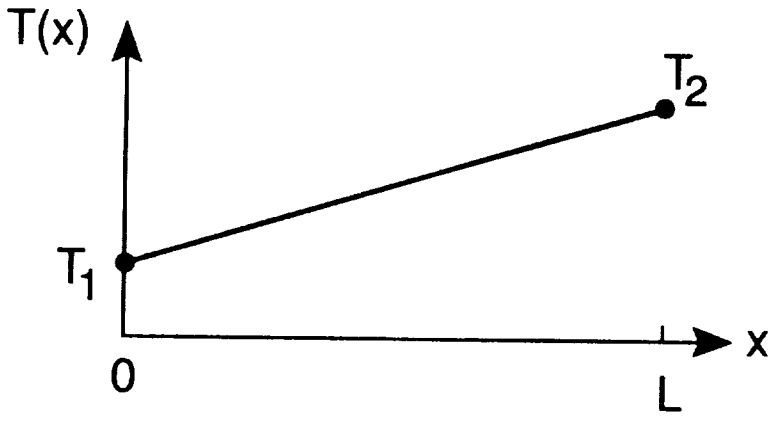

(b) Assumed temperature variation in a conventional linear element

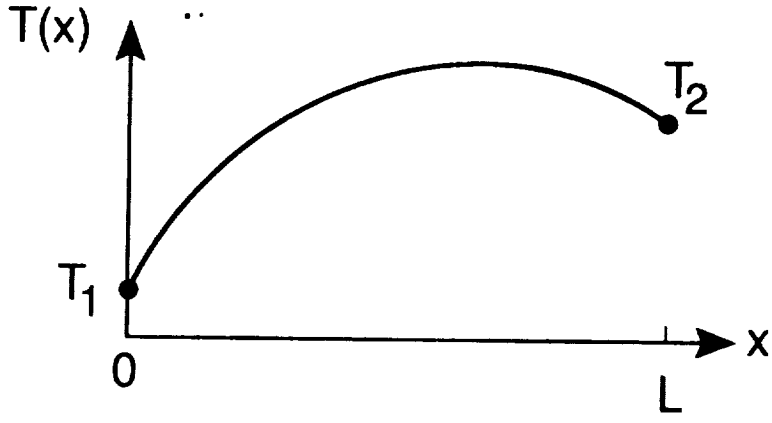

(c) Assumed temperature variation in a hierarchical nodeless variable element

Figure 2. One-dimensional thermal finite element and typical element temperature distributions.

$$T(x) = \sum_{i=1}^{3} N_i(x)T_i = \{N(x)\}^T \{T\} \tag{3.1}$$

where $\{T\}$ is the vector of unknown variables and $\{N(x)\}^T$ is the row vector of element interpolation functions. The nodal temperatures are T_1 and T_2, and T_3 is the nodeless variable. Similarly, in the structural analysis, the element displacement, u, is the unknown variable and is expressed in the form

$$u(x) = \sum_{i=1}^{3} N_i(x)u_i = \{N(x)\}^T \{u\} \tag{3.2}$$

where $\{u\}$ is the vector of unknown variables and $\{N(x)\}^T$ is the same row vector used to approximate the element temperature distribution. Once again, u_1 and u_2 are nodal displacements, and u_3 is the nodeless variable. The element interpolation functions for an element of length L are defined by

$$N_1 = 1 - \frac{x}{L}$$

$$N_2 = \frac{x}{L} \tag{3.3}$$

$$N_3 = \frac{x}{L}\left(1 - \frac{x}{L}\right)$$

where N_1 and N_2 are the nodal interpolation functions and N_3 is the nodeless variable interpolation function. Note that the nodeless variable does not represent the actual nodal temperature or displacement, but rather is directly related to the magnitude of the nonlinear variation of the element temperature

and displacement distributions. When the nodeless variable is constrained to be zero, the approximations of the element temperature and displacement distributions reduce to the conventional linear element approximation. For the hierarchical finite element formulation with one nodeless variable, a quadratic distribution of the unknown variables is assumed which is capable of representing the general solution more realistically.

3.2 Derivation of Flux-based Finite Element Equations

3.2.1 Thermal Analysis

The transient thermal response of a structure is governed by the energy equation. For a one-dimensional, uncoupled, thermal-structural analysis with no internal heat generation, the energy equation can be written in the form

$$\frac{\partial U}{\partial t} + \frac{\partial E}{\partial x} = 0 \tag{3.4}$$

The variable U, and the heat flux, E, are defined by

$$\frac{\partial U}{\partial t} = \rho c \frac{\partial T}{\partial t}$$

$$E = q_x = -k \frac{\partial T}{\partial x} \tag{3.5}$$

where T is the temperature, ρ is the material density, c is the specific heat, and k is the thermal conductivity. Both specific heat and thermal conductivity may be temperature dependent.

The Taylor-Galerkin algorithm is applied to the governing equation, equation (3.4). A Taylor series expansion of the variable U(x,t) in time is needed to establish recursion relations. The Taylor series expansion of U(x,t) in time is in the form of an infinite series

$$U(x,t^{n+1}) = U(x,t^n) + \frac{\partial U}{\partial t}(t^{n+1} - t^n) + \frac{1}{2!}\frac{\partial^2 U}{\partial t^2}(t^{n+1} - t^n)^2 + \frac{1}{3!}\frac{\partial^3 U}{\partial t^3}(t^{n+1} - t^n)^3 + \cdots \tag{3.6}$$

The change in the variable U with respect to time is defined as

$$\Delta U = U^{n+1} - U^n \tag{3.7}$$

For the first order accurate approximation in time, the change in the variable U is approximated as

$$\Delta U = \frac{\partial U^n}{\partial t}\Delta t \tag{3.8}$$

Substituting for the first derivative of the variable U from equation (3.4), equation (3.8) becomes

$$\Delta U + \Delta t \frac{\partial E^n}{\partial x} = 0 \tag{3.9}$$

The Galerkin method of weighted residuals is now applied to minimize the error of the approximation of the dependent variable over the element length,

$$\int_L N_i \, R \, dx = 0 \tag{3.10}$$

where N_i, the interpolation functions, are used as the weighting functions and R is the residual. For the nodeless variable formulation, i = 1 to 3, establishing three equations for minimizing the error of the three unknown variables. By substituting equation (3.9) for the residual, where R equals the left hand side of equation (3.9), equation (3.10) becomes

$$\int_L N_i \, \Delta U \, dx + \Delta t \int_L N_i \frac{\partial E^n}{\partial x} dx = 0 \tag{3.11}$$

Integration by parts on the second term in equation (3.11) yields

$$\int_L N_i \, \Delta U \, dx = \Delta t \int_L \frac{\partial N_i}{\partial x} E^n \, dx - \Delta t \left(N_i(0) \, E^n(0) - N_i(L) \, E^n(L) \right) \tag{3.12}$$

The finite element approximations are now needed for discretization in space. Since the variable U is directly related to temperature, it follows from equation (3.1) that

$$\Delta U(x) = \sum_{i=1}^{3} N_i(x) \, \Delta U_i = \{N(x)\}^T \{\Delta U\} \tag{3.13}$$

where

$$\Delta U_i = \rho \, c \, \Delta T_i = \rho \, c \, (T_i^{n+1} - T_i^n) \tag{3.14}$$

The flux-based assumption discretizes the heat flux in the same form as the variable U, where heat flux E^n replaces ΔU in equation (3.13). The nodal

values of heat flux, E_1 and E_2, are related to the temperature gradients through Fourier's law. Since heat flux is related to the gradient of the temperature, and the temperature distribution is assumed to be quadratic, the assumed heat flux must be a linear distribution, requiring that the nodeless variable heat flux, E_3, must be zero. Thus the heat flux distribution reduces to a linear distribution in the form

$$E^n(x) = \sum_{i=1}^{2} N_i(x)\, E_i^n = \{\overline{N(x)}\}^T \{E\}^n \tag{3.15}$$

where $\{E\}^n$ is the nodal heat flux vector and $\{\overline{N(x)}\}^T$ is the row matrix of the linear interpolation functions N_1 and N_2. The vector $\{\Delta U\}$ and heat flux nodal vectors are independent of the integration over the element length. The finite element approximations, equations (3.13 and 3.15), are substituted into equation (3.12) to yield the finite element equation in the form

$$[M]\{\Delta U\} = \Delta t\, [D]\, \{E\}^n - \Delta t\, \{B_T\} \tag{3.16}$$

where [M] denotes the matrix

$$[M] = \int_L \{N\}\{N\}^T dx \tag{3.17}$$

The first term of the right hand side of equation (3.16) is associated with the heat flux within the element, and $\{B_T\}$ is the boundary term associated with the heat flux across the element boundaries. The matrix [D] and vector $\{B_T\}$ are defined by

$$[D] = \int_L \frac{\partial \{N\}}{\partial x} \{ \overline{N(x)} \}^T \, dx \tag{3.18}$$

$$\{B_T\} = \begin{Bmatrix} -q(x = 0) \\ q(x = L) \\ 0 \end{Bmatrix} \tag{3.19}$$

where q in equation (3.19) represents the thermal boundary conditions and is replaced by any one of the several different types of boundary conditions given in equation (2.17). The closed-form expressions for the terms in matrix [M] and [D] are given in Appendix A.

The nodal heat flux vector in equation (3.16) is related to the nodal temperatures through Fourier's law and the finite element approximation for temperature. The terms in the vector are evaluated at the corresponding nodes where x = 0 at node 1 and x = L at node 2. The vector is defined by

$$\{E\}^n = \begin{Bmatrix} \left(-k \frac{\partial \{N\}^T}{\partial x} \{T\}^n \right) \Big|_{\text{node 1}} \\ \left(-k \frac{\partial \{N\}^T}{\partial x} \{T\}^n \right) \Big|_{\text{node 2}} \end{Bmatrix} \tag{3.20}$$

where $|_{\text{node i}}$ symbolizes the evaluation of the quantity at node i. Since $\{E\}^n$ is dependent on nodal temperatures and the nodal values for thermal conductivity, k, it needs to be updated at every time step for transient thermal analyses. The matrix [D] is independent of thermal properties and needs only to be evaluated once, prior to the transient analysis. The finite element equation,

equation (3.16), is solved for ΔU at every time step. The nodal temperatures are determined from equation (3.14).

3.2.2 Structural Analysis

The one-dimensional quasi-static structural response is governed by the equilibrium equation written in the form

$$\frac{\partial E}{\partial x} = 0 \tag{3.21}$$

where E represents the element stress in the x-direction. The element stress is defined by

$$E = \sigma_1 - \sigma_2 \tag{3.22}$$

where σ_1 and σ_2 are the one-dimensional components of the stress vector associated with the displacement gradients and the temperature, respectively. The element stress, E, is related to displacement gradients and temperatures by Hooke's law for thermal stress problems. For one-dimensional problems, the stress components reduce to

$$\sigma_1 = E\frac{\partial u}{\partial x} \tag{3.23}$$

$$\sigma_2 = E\,\alpha\,(T(x) - T_o) \tag{3.24}$$

where E is the modulus of elasticity, u is the displacement in the x-direction, α is the coefficient of thermal expansion, T(x) is the temperature distribution, and T_o is the reference temperature for a zero stress state.

As with the thermal formulation, the Galerkin method of weighted residuals, equation (3.10) is applied to minimize the error of the approximation of the dependent variable over the element length. Here, the governing equation, equation (3.21), represents the residual, where R equals the left hand side of equation (3.21). Integration by parts is performed to produce an element integral term and a boundary integral term for application of applied stress boundary conditions. The resulting equation is in the form

$$\int_L \frac{\partial N_i}{\partial x} \sigma_1 \, dx - \int_L \frac{\partial N_i}{\partial x} \sigma_2 \, dx - \left(N_i(0)\, \sigma(0) - N_i(L)\, \sigma(L) \right) = 0 \qquad (3.25)$$

where i = 1 to 3 yields three equations for minimizing the error of the hierarchical finite element approximations. The finite element approximations are needed to discretize equation (3.25) in space. The finite element approximation of the displacement dependent variable is given in equation (3.2). For the structural formulation, the flux-based assumptions are applied to the stress components which are analogous to heat flux in the thermal formulation. The flux-based assumptions discretize the stress components in the same form as the dependent variable. The σ_1 component is a function of the displacement gradient, where the displacement distribution is assumed to be quadratic. The σ_1 stress component reduces to a linear approximation in the same manner that the flux approximation, which is a fuction of the temperature gradient, reduces to a linear approximation. Since the σ_2 stress component is directly dependent on temperatures and the temperature distribution approximation is quadratic, the approximation for σ_2 is also quadratic. The resulting stress component approximations are thus given by

$$\sigma_1(x) = \sum_{i=1}^{2} N_i(x)_i\sigma_{1i} = \{ \overline{N(x)} \}^T \{\sigma_1\} \tag{3.26}$$

$$\sigma_2(x) = \sum_{i=1}^{3} N_i(x)\sigma_{2i} = \{N(x)\}^T \{\sigma_2\} \tag{3.27}$$

where $\{ \overline{N(x)} \}^T$ is the row matrix of the linear interpolation function, $\{\sigma_1\}$ is the vector of nodal values for the stress component associated with the displacement gradient, $\{N(x)\}^T$ is the row matrix of the interpolation functions given in equation (3.3), and $\{\sigma_2\}$ is a vector of known values associated with temperature and will be defined subsequently in the thesis. The flux-based assumptions, equations (3.26 and 3.27), are substituted into equation (3.25) to yield the finite element equation.

For a one-dimensional, quasi-static, structural analysis, the finite element equation is in the form

$$[D] \{\sigma_1\} = [D_2] \{\sigma_2\} + \{B\} \tag{3.28}$$

where the matrix [D] is identical to the matrix [D] produced in the thermal formulation, and is defined by equation (3.18). The matrix $[D_2]$ associated with the σ_2 stress component and the vector {B} associated with the boundary conditions are defined by

$$[D_2] = \int_L \frac{\partial\{N\}}{\partial x} \{N\}^T dx \tag{3.29}$$

$$\{B\} = \begin{Bmatrix} -\sigma(x = 0) \\ \sigma(x = L) \\ 0 \end{Bmatrix} \tag{3.30}$$

where σ in equation (3.30) represents an applied stress boundary condition. The expressions for the terms in the finite element matrix $[D_2]$ are given in Appendix A.

The terms in the vector $\{\sigma_1\}$ are related to nodal displacements through equation (3.23) and the finite element approximation for displacements, equation (3.2). The vector $\{\sigma_1\}$ is defined by

$$\{\sigma_1\} = \begin{Bmatrix} \left(E\frac{\partial\{N\}^T}{\partial x}\{u\}\right)\Big|_{\text{node 1}} \\ \left(E\frac{\partial\{N\}^T}{\partial x}\{u\}\right)\Big|_{\text{node 2}} \end{Bmatrix} \tag{3.31}$$

where the gradients of the interpolation functions given in equation (3.3), evaluated at the nodes, are substituted into equation (3.31). The displacements in equation (3.31) are extracted to yield the $\{\sigma_1\}$ stress component in the form

$$\{\sigma_1\} = [P]\{u\} \tag{3.32}$$

The $\{\sigma_1\}$ nodal stress component vector is given here in terms of the unknown displacement vector, $\{u\}$, and a matrix, $[P]$, which is a function of the element length and the modulus of elasticity. The coefficients in the matrix $[P]$ are given in Appendix A. The expression for the stress vector $\{\sigma_1\}$, is substituted into the finite element equation, equation (3.28), which can now be written in terms of the unknown displacement vector.

The vector $\{\sigma_2\}$ is derived by equating the flux-based assumption for σ_2, given in equation (3.27), with the definition of σ_2 given in equation (3.24), where T(x) is replaced by the finite element approximation for T(x), equation (3.1). The expression is written in the form

$$\sum_{i=1}^{3} N_i(x)\sigma_{2i} = E\,\alpha\,(\sum_{i=1}^{3} N_i(x)T_i - T_o) \tag{3.33}$$

Evaluating equation (3.33) at the element nodes where i = 1 and i = 2 , and x = 0 and x = L, respectively, gives the values of the vector $\{\sigma_2\}$ as

$$\{\sigma_2\} = \begin{Bmatrix} E\alpha\,(T_1 - T_o) \\ E\alpha\,(T_2 - T_o) \\ E\alpha\,T_3 \end{Bmatrix} \tag{3.34}$$

The stress component vector, $\{\sigma_2\}$, is a vector of known quantities because the element nodal temperatures T_1 and T_2, and the element thermal nodeless variable T_3 are obtained from the thermal analysis.

3.3 Thermal-Structural Analysis Algorithm

The hierarchical flux-based finite element analysis method is implemented in a computer program for performing transient thermal and quasi-static structural analyses. A flow chart for the one-dimensional thermal-structural finite element analysis method is shown in figure 3. Once the finite element model is input, the finite element matrices [D] and $[D_2]$ are assembled

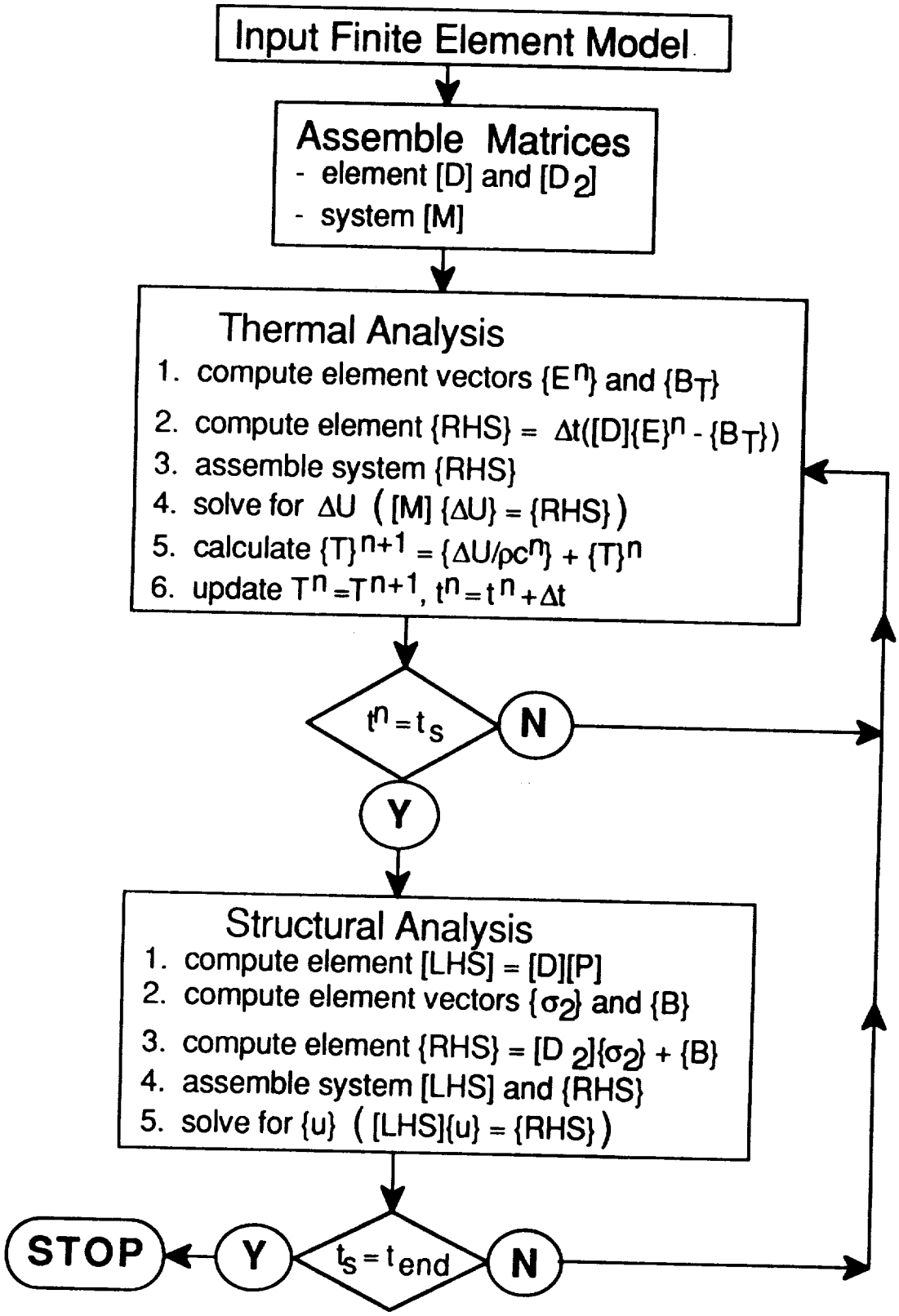

Figure 3. Flow chart for one-dimensional hierarhical flux-based thermal-structural analysis.

along with the system [M] matrix. The thermal analysis is performed first and consists of: (1) computing the element vectors $\{E^n\}$ and $\{B_T\}$; (2) computing the element right hand side vectors, where {RHS} is the right hand side of equation (3.16); (3) assembling the system {RHS}; (4) solving the system equations for $\{\Delta U\}$; (5) computing the $\{T\}^{n+1}$ vector from equation (3.14); and (6) updating the temperatures and time step for proceeding in a transient thermal analysis. If the time $t^n = t_s$, where t_s in the time set for a quasi-static structural analysis, the structural analysis begins and the vector $\{T\}^n$ is used for thermal loading. The structural analysis consists of: (1) computing the element [LHS] matrix, where [LHS] represents the left hand side matrix of the finite element equation ([LHS] = [D][P]); (2) computing the element vectors $\{\sigma_2\}$ and {B}; (3) computing the element {RHS}, where {RHS} represents the right hand side of equation (3.28); (4) assembling the system [LHS] and {RHS}; and (5) solving for the vector {u}. If $t_s = t_{end}$, where t_{end} is the time set to end the thermal-structural analysis, the analysis is complete.

3.4 Applications of One-Dimensional Methodologies

To evaluate the hierarchical flux-based finite element method, four one-dimensional thermal and structural problems are presented. The first two example problems are for the transient thermal analysis of a copper slab with constant material properties and with temperature dependent material properties. The following two example problems are for the thermal and structural analysis of a copper rod with one end constrained and with both ends constrained. Results obtained by the hierarchical flux-based method are

compared with solutions obtained using the conventional method and available exact solutions.

3.4.1 Transient Thermal Analysis of a Copper Slab

A copper slab 0.02 in. in length subjected to an applied heating rate of 200 Btu/in.^{2}-sec on the face at x = 0 and a prescribed temperature equivalent to the initial temperature at x = L is analyzed for two cases: (1) constant material properties and an initial temperature of T_i = 0 °F; and (2) temperature dependent thermal conductivity and an initial temperature of T_i = -410 °F. A schematic diagram of the finite element model and the material properties for copper are shown in figure 4.

For case one, with constant material properties, the exact solution to the governing equation for one-dimensional transient heat transfer can be derived from the method of separation of variables and is in the form of an infinite series [20]. The exact solution for the transient temperature distribution is given by

$$T(x,t) = \frac{q(L-x)}{k} - \frac{8qL}{k\pi^2} \sum_{n=0}^{\infty} \frac{(-1)^n}{(2n+1)^2} \sin \frac{(2n+1)\,\pi\,(L-x)}{2L} \exp\left(\frac{-k}{\rho c}\left[\frac{(2n+1)\,\pi}{2L}\right]^2 t\right) \tag{3.35}$$

where the boundary conditions and initial condition are

$$\begin{aligned} -k\frac{\partial T}{\partial x}(0,t) &= q \\ T(L,t) &= 0 \\ T(x,0) &= 0 \end{aligned} \tag{3.36}$$

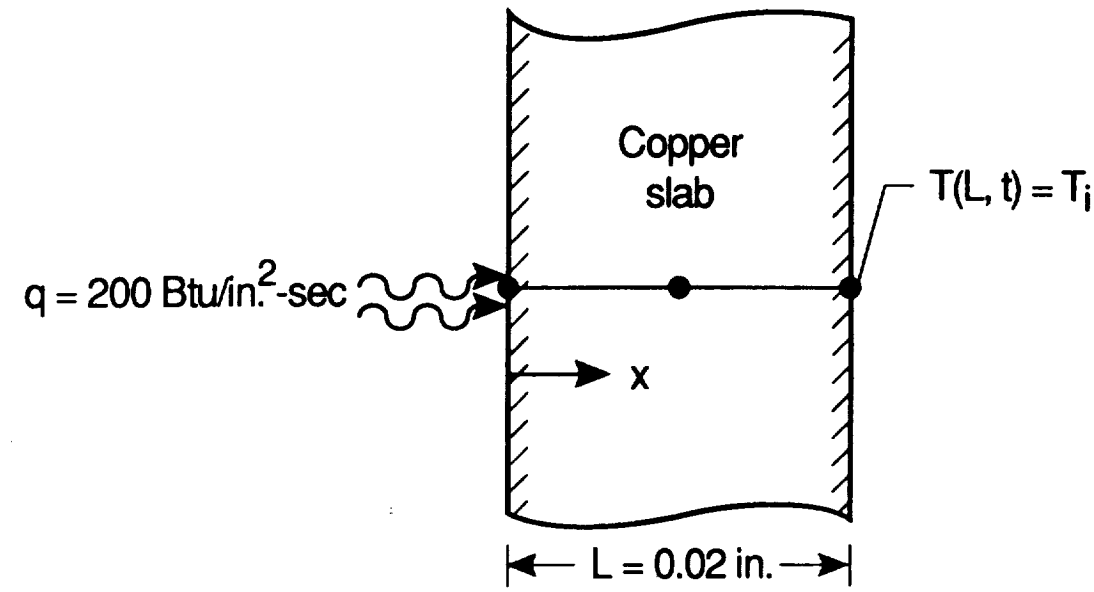

(a) Schematic diagram of thermal finite element model

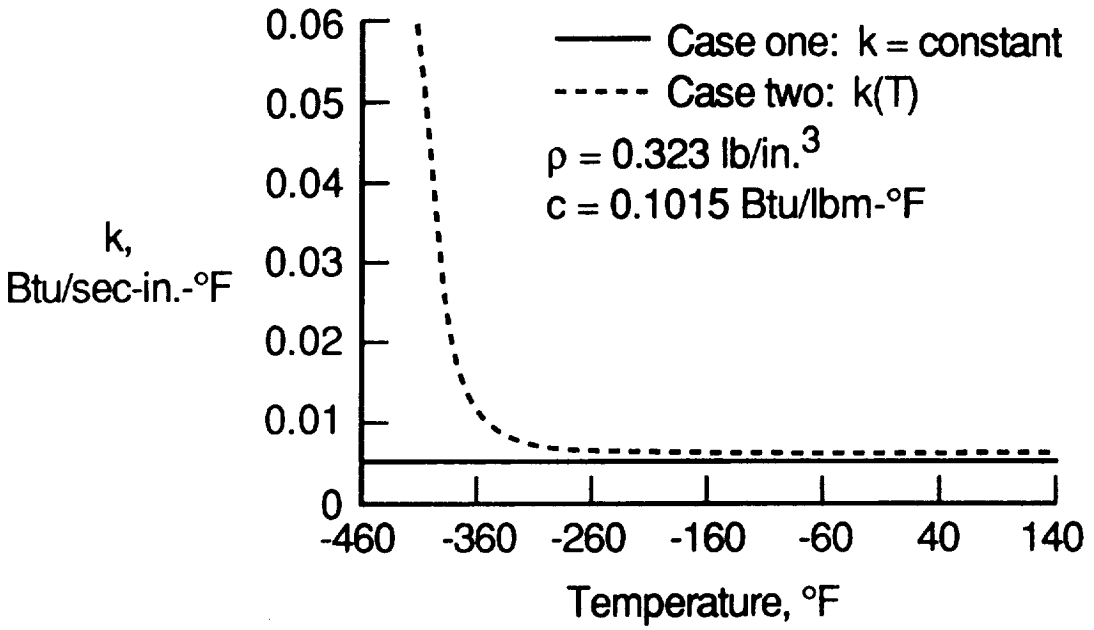

(b) Material properties for copper

Figure 4. Schematic diagram of thermal finite element model of a copper slab and material properties for copper.

The temperature distributions within the slab obtained from the exact solution are shown in figure 5 at two times during the transient thermal response. Also shown in figure 5 are the finite element solutions obtained from the hierarchical flux-based and conventional methods. The flux-based method yields an accurate prediction of the exact solution using two nodeless variable elements, whereas the conventional method required the use of ten elements to obtain a temperature distribution prediction within one percent of the exact solution, not shown. The overall average error between the finite element and exact temperature distributions is defined by

$$\text{error} = \frac{\|e\|}{\|T\|} \times 100\ \% \tag{3.37}$$

where

$$\| e \|^2 = \frac{1}{L} \int_0^L (T_{exact} - T_{FE})^2\, dx$$

and

$$\| T \|^2 = \frac{1}{L} \int_0^L (T_{exact})^2\, dx$$

where T_{exact} is the exact temperature distribution and T_{FE} is the finite element temperature distribution over the length, L, of the finite element model. Using two elements with the conventional method results in a 29% overall average error at t = 0.0001 sec. and a 3% overall average error at t=0.001 sec. As shown in figure 5, the hierarchical finite element method provides a more accurate prediction of the temperature distribution than the conventional method for the same number of elements, especially at early times in the transient solution when there is a large temperature gradient within the slab.

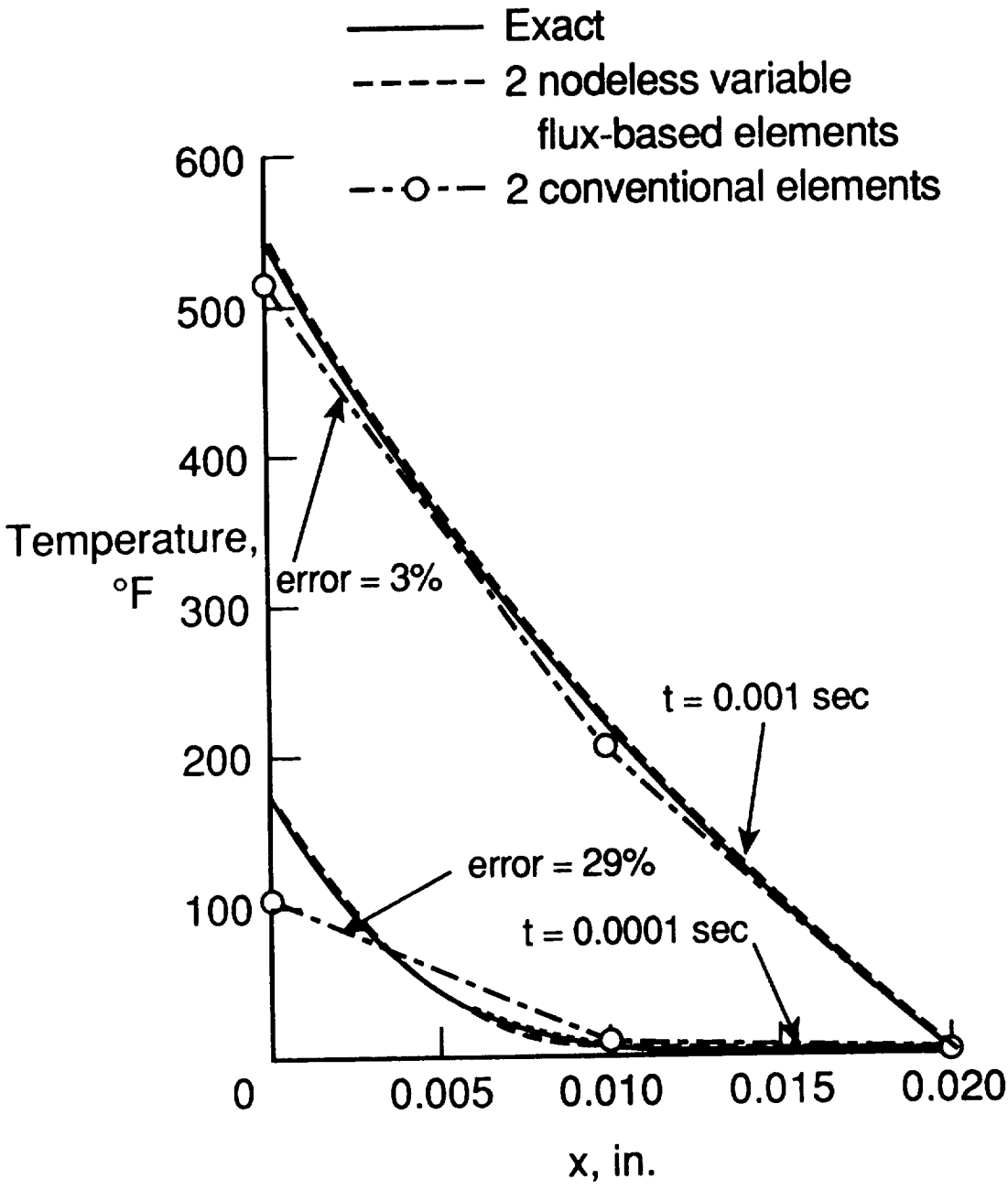

Figure 5. Case one: Temperature distributions in a copper slab with constant material properties.

For case two with temperature-dependent thermal conductivity, an initial temperature of T_i = -410 °F is used. At this low initial temperature, the thermal conductivity of copper is highly nonlinear as shown in figure 4. The transient thermal response of the copper slab, using the temperature dependent conductivity shown in figure 4, is predicted using both the hierarchical flux-based and conventional methods. Two temperature distributions are shown in figure 6 for t = 0.0001 sec. during the transient thermal analysis. Ten conventional elements are necessary for the temperature distribution to converge to within one percent of the temperature distribution obtained using eight conventional elements. The ten-conventional-element temperature distribution was then used as a reference solution. The hierarchical flux-based method predicted an accurate temperature distribution, within one percent of the reference solution, using only four nodeless variable elements. From the two examples presented above, the hierarchical flux-based method provides accurate temperature distributions using fewer elements.

3.4.2 Thermal-Structural Analysis of a Copper Rod

A copper rod one inch in length is analyzed for the transient thermal and quasi-static structural response at t = 0.5 sec. A schematic diagram of the thermal and structural finite element models for the two cases analyzed are shown in figure 7. In both cases, shown in figure 7(a), the thermal analysis consists of an applied aerodynamic heating rate of q = 10 Btu/in.^{2}-sec at x = 0 and a prescribed temperature equal to the initial temperature of 70 °F at x = L. The temperature distributions obtained using the exact solution, the hierarchical flux-base method, and the conventional method are shown in figure 8 for t = 0.5 sec. As can be observed from figure 8, two hierarchical flux-based elements

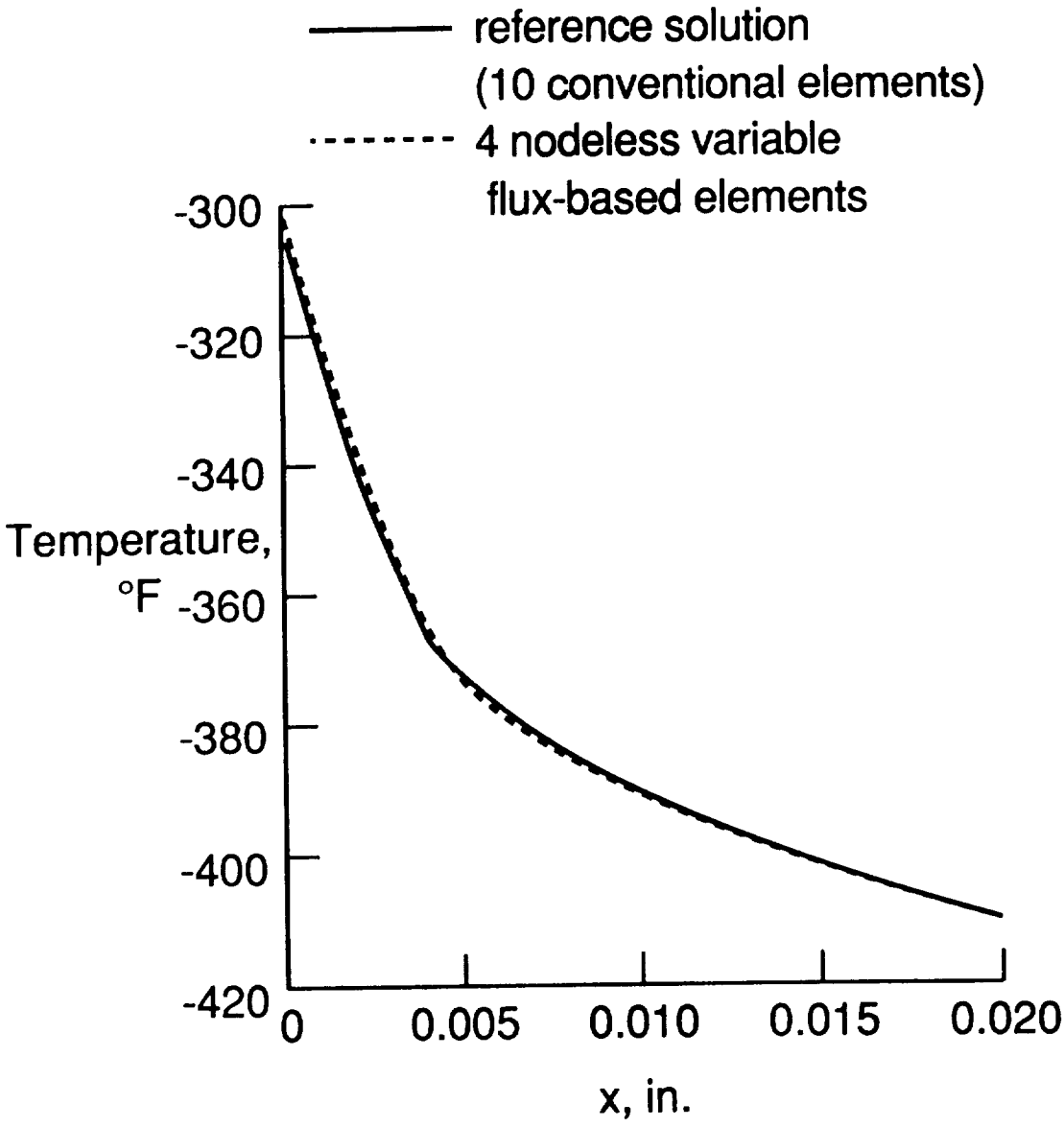

Figure 6. Case two: Temperature distributions in a copper slab with temperature dependent conductivity at t = 0.0001 sec.

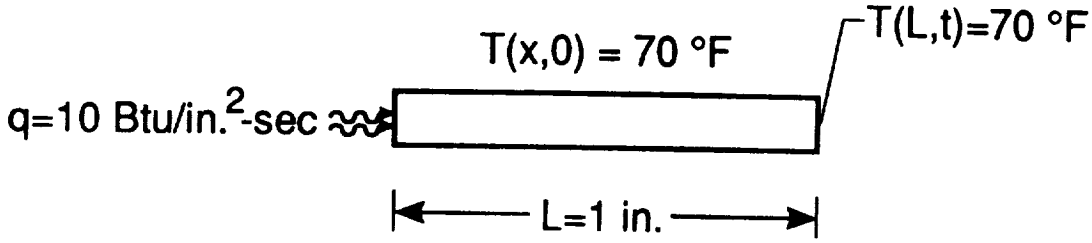

(a) Thermal boundary and initial conditions

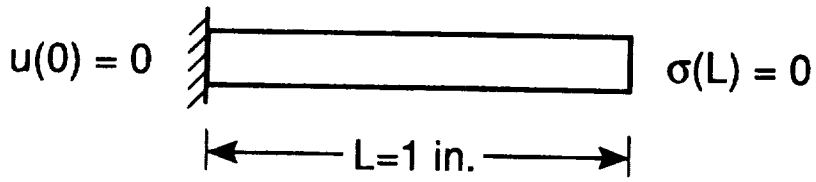

(b) Case one: structural boundary conditions, free end

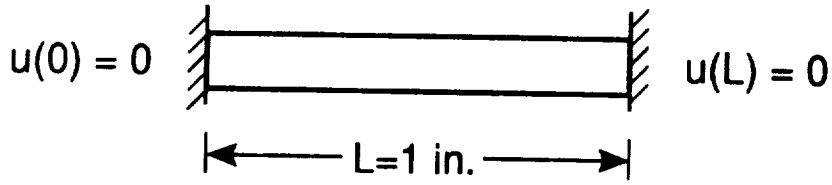

(c) Case two: structural boundary conditions, fixed ends

Figure 7. Schematic diagrams of thermal and structural finite element models of a copper rod.

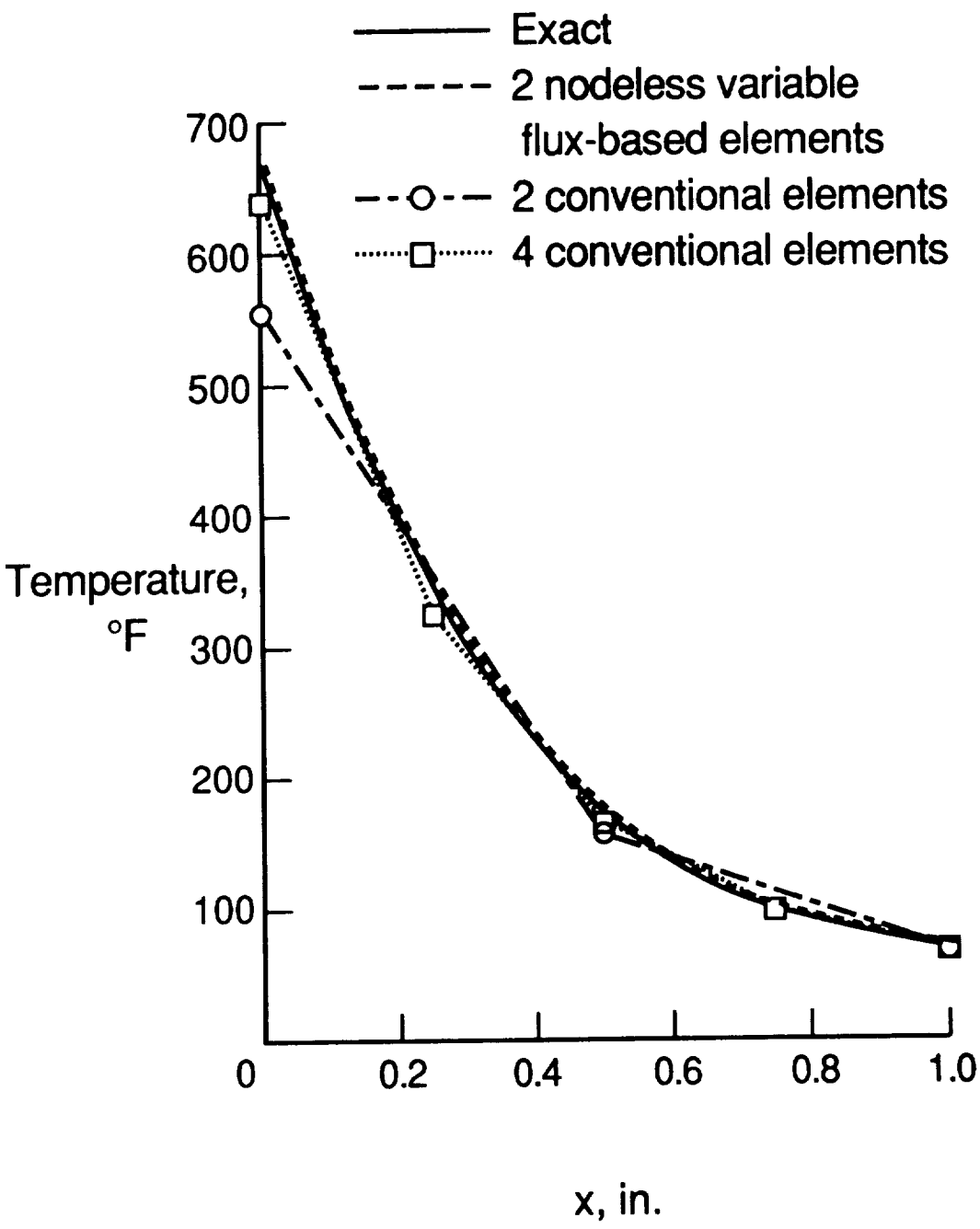

Figure 8. Temperature distributions in a copper rod at t = 0.5 sec.

are sufficient to predict the temperature distribution accurately, whereas four conventional elements are required to closely represent the exact solution.

Two quasi-static structural analysis cases are investigated using the temperature distributions shown in figure 8 at t = 0.5 sec. The structural boundary conditions for case one, shown in figure 7(b), constrains the end at x = 0 and allows for free expansion at x = L. The initial temperature of T_i = 70 °F from the thermal analysis was used as the reference temperature for a zero stress state, T_o = 70 °F. The displacement distributions obtained for case one using the exact solution, the hierarchical flux-based method, and the conventional method are shown in figure 9. Once again, four conventional elements are needed to closely approximate the exact solution whereas only two hierarchical flux-based elements are sufficient to provide accurate results. The next case investigated, case two, assumes both ends are constrained as shown in figure 7(c) and a reference temperature of T_o = 70 °F for a zero stress state.

The displacement distributions and the average element stresses obtained for case two are shown in figure 10(a) and figure 10(b), respectively. As shown in figure 10(a), two hierarchical flux-based elements were needed to closely represent the exact solution, whereas two conventional elements were insufficient to predict the displacement distribution accurately. The use of two conventional elements underpredicts the maximum displacement by 13 % whereas two nodeless variable elements overpredicts the maximum displacement by only 3.4 %. Using two conventional elements resulted in a 3% error in predicting the stress distribution in the copper rod whereas two hierarchical elements predicted the stress distribution within a 1 % error margin.

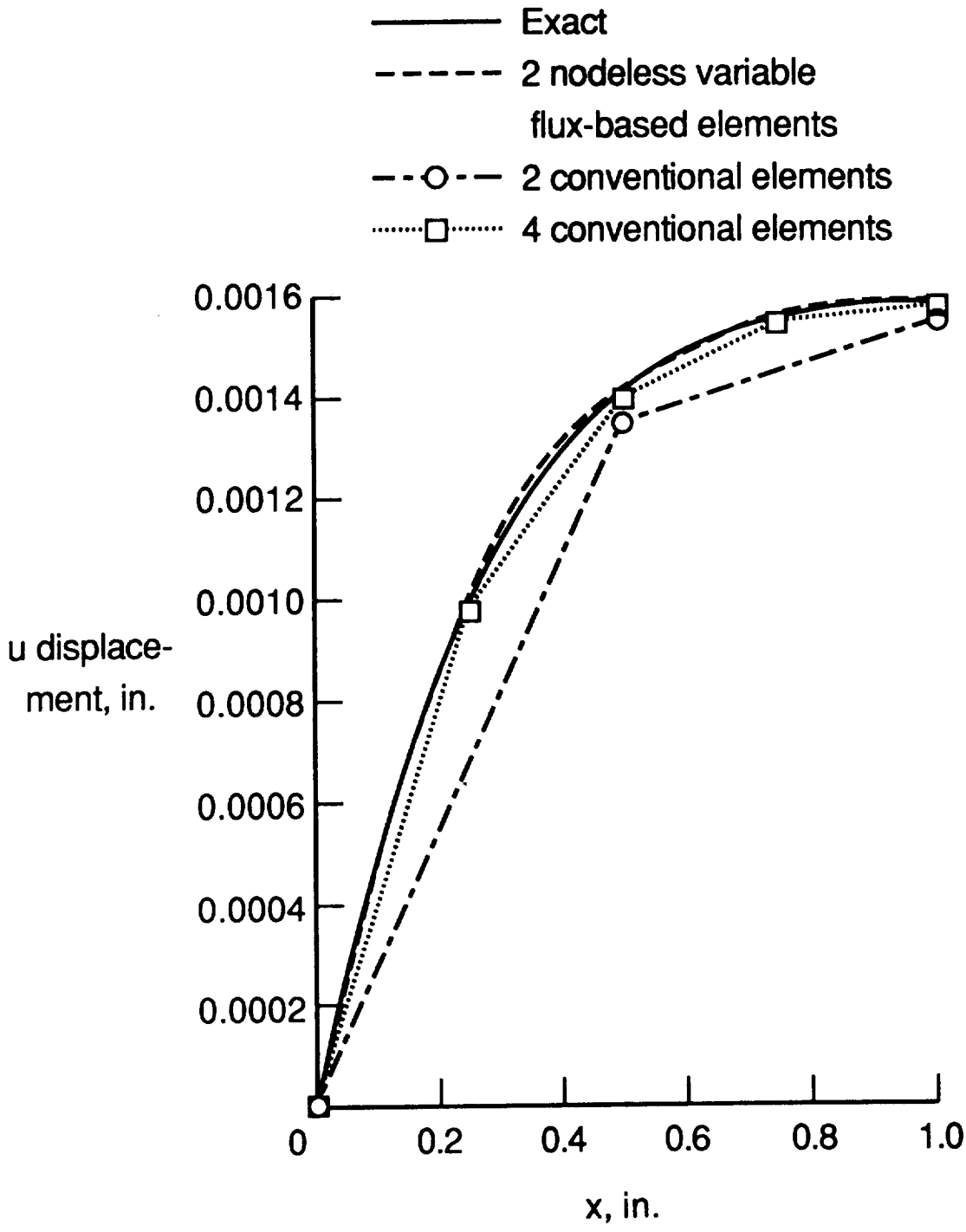

Figure 9. Case one: Displacement distributions in a copper rod subjected to thermal loading and constrained at x = 0 (t = 0.5 sec.).

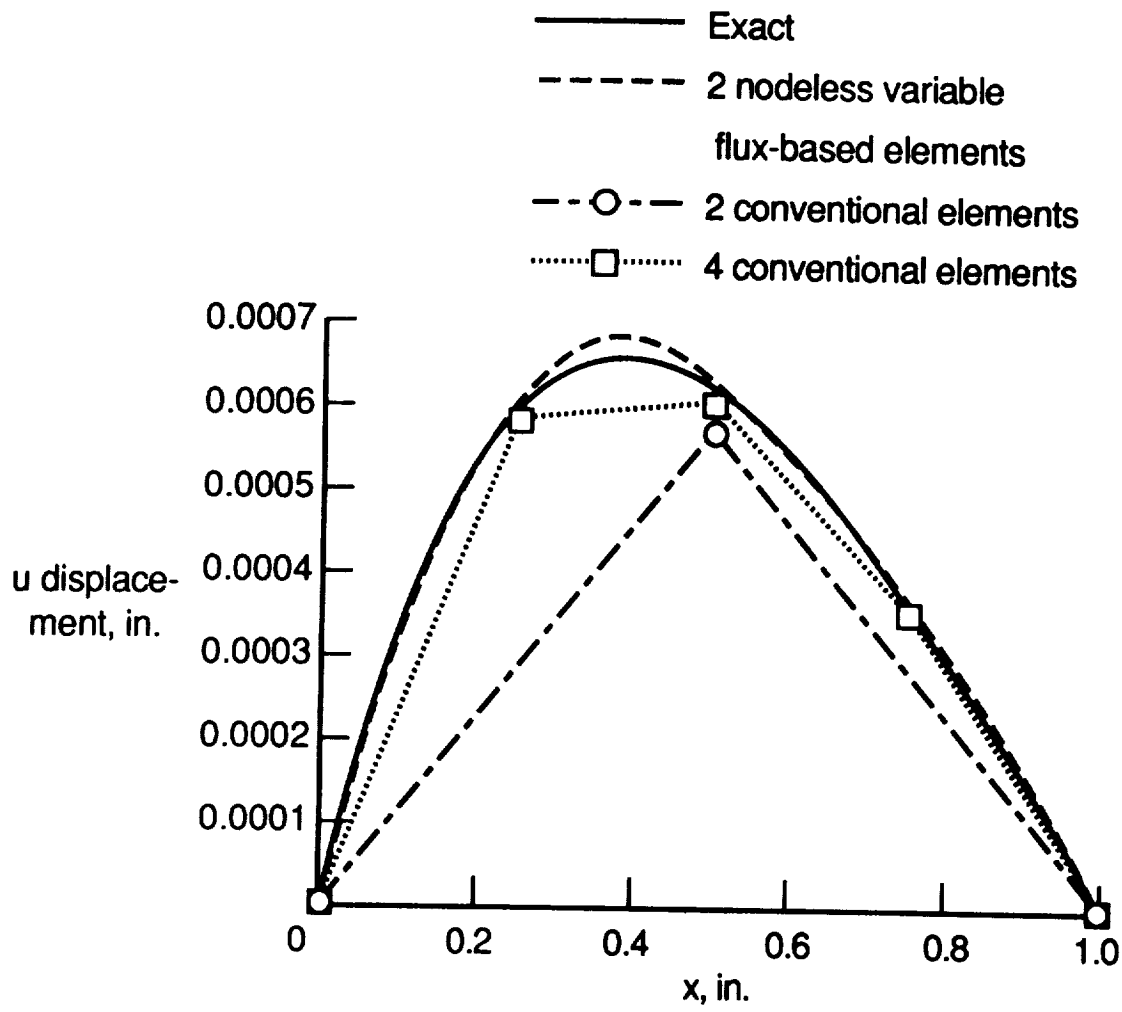

(a) Displacement distributions

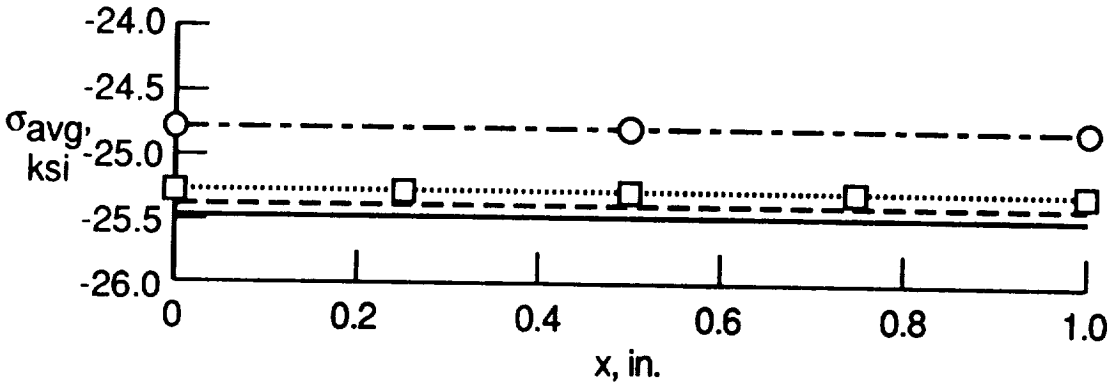

(b) Average stress

Figure 10. Case two: Structural response for a copper rod with both ends constrained.

The previous examples demonstrate the ability of the hierarchical method to predict accurate thermal and structural responses using fewer elements than required by the conventional method to obtain the same accuracy. The following chapter includes the extension of the hierarchical flux-based method for two-dimensional thermal-structural analyses.

Chapter 4
TWO-DIMENSIONAL NODELESS VARIABLE FINITE ELEMENTS USING FLUX-BASED FORMULATION

4.1 Element Interpolation Functions

In this chapter, the flux-based method is extended to develop a two-dimensional finite element formulation using nodeless variables. As with the conventional two-dimensional bilinear element formulation, a general quadrilateral element shape is employed for formulating the nodeless variable element interpolation functions. To simplify the element integrations arising in the finite element matrices, the transformation from Cartesian to natural coordinates shown in figure 1 is utilized. The relation between the two coordinate systems given in equation (2.9) is applied in the development of the two-dimensional finite element equations with nodeless variables.

For the hierarchical method, a nonlinear variation of the dependent variable is assumed over the element surface. Preserving the four-noded quadrilateral element, the nonlinear variation is established by introducing additional degrees of freedom in the approximation of the dependent variable. For the thermal analysis formulation, the distribution of temperature over the element surface is assumed in the form

$$T = \sum_{i=1}^{8} N_i(\zeta,\eta)\, T_i(t) = \{N(\zeta,\eta)\}^T \{T(t)\} \tag{4.1}$$

where $\{N(\zeta,\eta)\}^T$ is the row matrix of element interpolation functions and $\{T(t)\}$ is the vector of unknown variables. The nodal temperatures are T_1 through T_4, and the nodeless variables are T_5 through T_8. For the structural analysis formulation, the displacement distributions are assumed in the same form

$$u = \sum_{i=1}^{8} N_i(\zeta,\eta)\, u_i = \{N(\zeta,\eta)\}^T \{u\} \tag{4.2}$$

$$v = \sum_{i=1}^{8} N_i(\zeta,\eta)\, v_i = \{N(\zeta,\eta)\}^T \{v\} \tag{4.3}$$

where u and v are the displacements in the x- and y-coordinate directions, respectively. The vectors of unknown variables, {u} and {v}, contain the four nodal displacements and four nodeless variables. The displacement distributions can be expressed in a combined form as

$$\begin{Bmatrix} u \\ v \end{Bmatrix} = [N]\{\delta\} \tag{4.4}$$

where [N] is the combined matrix of interpolation functions for the structural formulation and $\{\delta\}$ is the vector of nodal displacements and nodeless variables. These matrices, [N] and $\{\delta\}$, are defined by

$$[N] = \begin{bmatrix} N_1 & 0 & N_2 & 0 & \cdots & N_8 & 0 \\ 0 & N_1 & 0 & N_2 & \cdots & 0 & N_8 \end{bmatrix} \tag{4.5}$$

$$\{\delta\} = \begin{Bmatrix} u_1 \\ v_1 \\ u_2 \\ v_2 \\ \cdot \\ \cdot \\ \cdot \\ u_8 \\ v_8 \end{Bmatrix} \tag{4.6}$$

The element interpolation functions, N_i, i = 1 to 4 are identical to those used for the conventional bilinear four-node element given in equation (2.10), and N_i, i = 5 to 8 are the nodeless variable interpolation functions given by

$$\begin{aligned} N_5 &= \frac{1}{8}(1-\zeta^2)(1-\eta) \\ N_6 &= \frac{1}{8}(1+\zeta)(1-\eta^2) \\ N_7 &= \frac{1}{8}(1-\zeta^2)(1+\eta) \\ N_8 &= \frac{1}{8}(1-\zeta)(1-\eta^2) \end{aligned} \tag{4.7}$$

where each interpolation function varies quadratically along one edge and vanishes along the other edges of the element.

Utilizing the nodeless variable interpolation functions in equations (4.1 - 4.3) provides a quadratic variation of the temperature or displacement distribution over the element with only four element nodes. A schematic of typical element temperature distributions for the nodeless variable element and conventional element are shown in figure 11. The magnitude of the nonlinear variation on an element edge depends on the magnitude of the nodeless variables. If the nodeless variables are constrained to zero in the approximation of the temperature or displacement distribution given in

equations (4.1 - 4.3), the distribution reduces to the conventional bilinear element approximation.

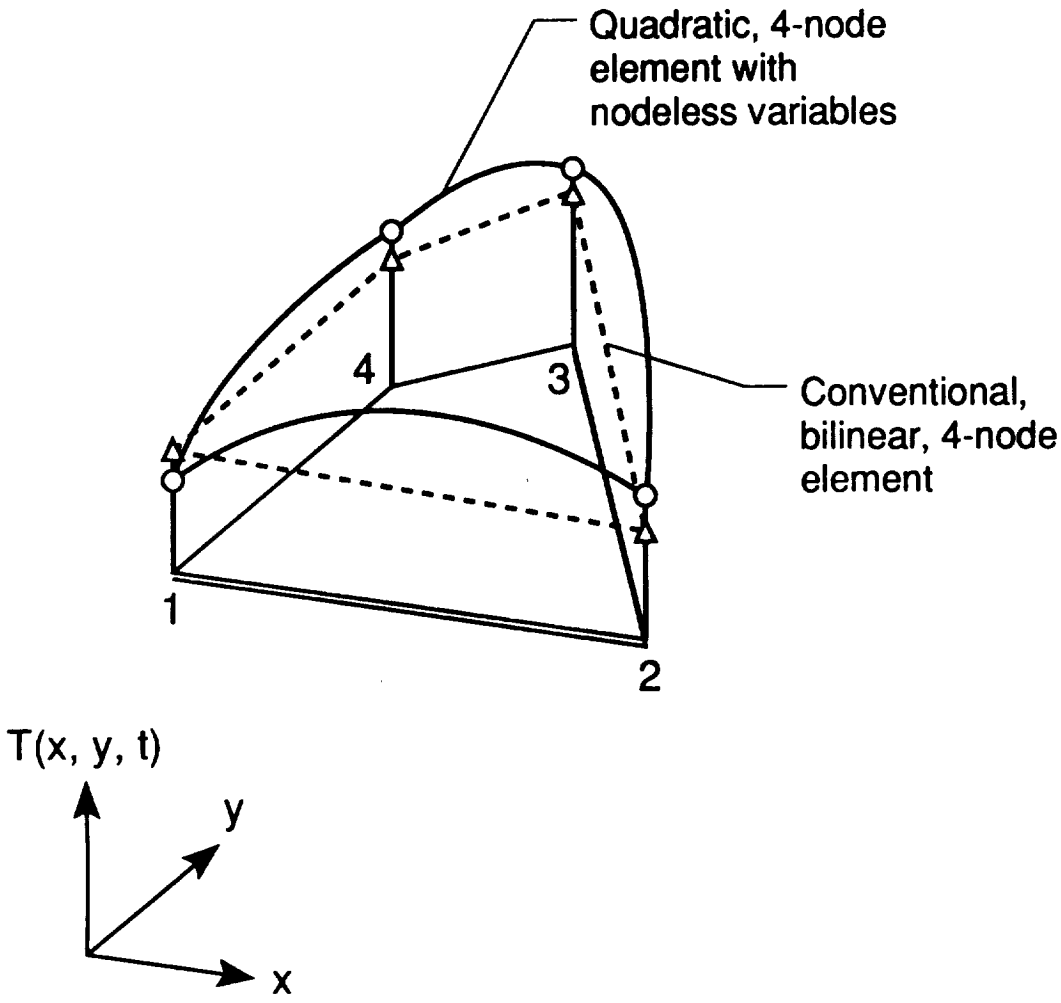

Figure 11. Typical two-dimensional finite element temperature distributions.

4.2 Derivation of Flux-based Finite Element Equation

4.2.1 Thermal Analysis

The transient thermal response for a two-dimensional uncoupled thermal-structural analysis is governed by the energy equation given in equation (2.1), where the terms in the equation are defined in equation (2.2). The flux-based Taylor-Galerkin algorithm is applied to the governing equation to yield the finite element equations. As with the one-dimensional formulation, the Taylor series approximation for the variable ΔU, equations (3.6 - 3.8), is utilized to establish recursion relations. The approximation, equation (3.8) is substituted in the two-dimensional governing equation, equation (2.1), to yield

$$\Delta U + \Delta t \frac{\partial E^n}{\partial x} + \Delta t \frac{\partial F^n}{\partial y} = 0 \tag{4.8}$$

The Galerkin method of weighted residuals is applied to minimize the error of the finite element approximations over the element area,

$$\int_A N_i \, R \, dA = 0 \tag{4.9}$$

where N_i, the nodeless variable element interpolation functions, are used as the weighting functions and R is the residual. For the quadrilateral nodeless variable element, i = 1 to 8, establishing eight equations for minimizing the error of the eight unknown variables. The left hand side of equation (4.8) is substituted for the residual to yield

$$\int_A N_i \, \Delta U \, dA + \Delta t \int_A N_i \frac{\partial E^n}{\partial x} dA + \Delta t \int_A N_i \frac{\partial F^n}{\partial y} dA = 0 \tag{4.10}$$

Integration by parts is performed on the second and third terms in equation (4.10) to yield

$$\int_A N_i \, \Delta U \, dA = \Delta t \int_A \frac{\partial N_i}{\partial x} E^n \, dA + \Delta t \int_A \frac{\partial N_i}{\partial y} F^n \, dA - \Delta t \int_S N_i \, q_n \, dS \qquad (4.11)$$

where the first two terms on the right hand side represent the heat conduction within the element and the last term on the right hand side represents the heat flux across the element boundaries. The quantity q_n is the heat flux normal to the element boundary.

The next step in the formulation of the thermal finite element equation is to discretize equation (4.11) in space by implementing the finite element approximations. The variable, ΔU, being directly related to temperature, is discretized in the same form as equation (4.1) and is given by

$$\Delta U = \sum_{i=1}^{8} N_i(\zeta,\eta) \, \Delta U_i = \{N(\zeta,\eta)\}^T \{\Delta U\} \qquad (4.12)$$

where

$$\Delta U_i = \rho \, c \, \Delta T_i = \rho \, c \, (T_i^{n+1} - T_i^n) \qquad (4.13)$$

The flux-based assumptions discretize the heat flux in the x- and y-coordinate directions in the same form as the dependent variable. As with the one-dimensional formulation, the variations of heat flux over the element surface reduce to bilinear approximations in the form

$$E^n = \sum_{i=1}^{4} N_i(\zeta,\eta) \, E_i^n = \{ \overline{N(\zeta,\eta)} \}^T \{E^n\} \qquad (4.14)$$

$$F^n = \sum_{i=1}^{4} N_i(\zeta,\eta)\, F_i^n = \{\overline{N(\zeta,\eta)}\}^T \{F^n\} \qquad (4.15)$$

where $\{\overline{N(\zeta,\eta)}\}^T$ is the row matrix of linear interpolation functions given by equation (2.10), and $\{E^n\}$ and $\{F^n\}$ are the nodal heat flux vectors in the x- and y-coordinate directions, respectively.

The two-dimensional transient thermal finite element equation can be written in matrix form as

$$[M]\{\Delta U\} = \Delta t\,[D_x]\{E^n\} + \Delta t\,[D_y]\{F^n\} - \Delta t\,[B]\{q\} \qquad (4.16)$$

where [M] denotes the matrix associated with $\{\Delta U\}$, $[D_x]$ and $[D_y]$ are associated with the heat transfer within the element, and [B] is the boundary matrix. These matrices are given by

$$[M] = \int_A \{N\}\{N\}^T dA \qquad (4.17)$$

$$[D_x] = \int_A \frac{\partial\{N\}}{\partial x}\{\overline{N}\}^T dA \qquad (4.18)$$

$$[D_y] = \int_A \frac{\partial\{N\}}{\partial y}\{\overline{N}\}^T dA \qquad (4.19)$$

$$[B] = \int_S \{N\}\{\overline{N}\}^T dS \qquad (4.20)$$

The transformation from Cartesian to natural coordinates used to evaluate these matrices requires relating the gradients of the interpolation functions in both coordinate systems. The chain rule is applied to obtain the relationship

$$\begin{Bmatrix} \frac{\partial N}{\partial \zeta} \\ \frac{\partial N}{\partial \eta} \end{Bmatrix} = \begin{bmatrix} \frac{\partial x}{\partial \zeta} & \frac{\partial y}{\partial \zeta} \\ \frac{\partial x}{\partial \eta} & \frac{\partial y}{\partial \eta} \end{bmatrix} \begin{Bmatrix} \frac{\partial N}{\partial x} \\ \frac{\partial N}{\partial y} \end{Bmatrix} = [J] \begin{Bmatrix} \frac{\partial N}{\partial x} \\ \frac{\partial N}{\partial y} \end{Bmatrix} \tag{4.21}$$

where [J] is the Jacobian matrix. Relating x and y to the natural coordinates using equation (2.9), [J] is given by

$$[J] = \begin{bmatrix} \sum_{i=1}^{4} \frac{\partial N_i}{\partial \zeta} x_i & \sum_{i=1}^{4} \frac{\partial N_i}{\partial \zeta} y_i \\ \sum_{i=1}^{4} \frac{\partial N_i}{\partial \eta} x_i & \sum_{i=1}^{4} \frac{\partial N_i}{\partial \eta} y_i \end{bmatrix} = \begin{bmatrix} J_{11} & J_{12} \\ J_{21} & J_{22} \end{bmatrix} \tag{4.22}$$

From equations (4.21 - 4.22), it follows that

$$\begin{Bmatrix} \frac{\partial N}{\partial x} \\ \frac{\partial N}{\partial y} \end{Bmatrix} = [J]^{-1} \begin{Bmatrix} \frac{\partial N}{\partial \zeta} \\ \frac{\partial N}{\partial \eta} \end{Bmatrix} = \frac{1}{|J|} \begin{bmatrix} J_{22} & -J_{12} \\ -J_{21} & J_{11} \end{bmatrix} \begin{Bmatrix} \frac{\partial N}{\partial \zeta} \\ \frac{\partial N}{\partial \eta} \end{Bmatrix} \tag{4.23}$$

where $[J]^{-1}$ is the inverse and $|J|$ is the determinate of the Jacobian matrix [J]. The derivatives of the interpolation function gradients occurring in equations (4.18 - 4.19) with respect to the Cartesian coordinates are replaced by the corresponding gradients in natural coordinates as

$$\frac{\partial N_i}{\partial x} = \frac{1}{|J|}\left(J_{22}\frac{\partial N_i}{\partial \zeta} - J_{12}\frac{\partial N_i}{\partial \eta}\right) \tag{4.24}$$

$$\frac{\partial N_i}{\partial y} = \frac{1}{|J|}\left(-J_{21}\frac{\partial N_i}{\partial \zeta} + J_{11}\frac{\partial N_i}{\partial \eta}\right) \tag{4.25}$$

Using the relationship $dA = |J|\, d\zeta\, d\eta$, the integration of the matrices given in equations (4.17 - 4.19) can now be evaluated with respect to natural coordinates over the square element area shown in figure 1. All matrices arising in the transient thermal finite element equation for the quadrilateral element, equation (4.16), can be evaluating in closed form. The evaluation of the matrices, equations (4.17 - 4.19), was greatly simplified by using Mathematica [21], a general purpose computer software system for performing algebraic manipulation. The closed form expressions for the coefficients in the two-dimensional transient thermal finite element matrices and the evaluation of $|J|$ are given in Appendix B.

The nodal heat flux vectors, $\{E^n\}$ and $\{F^n\}$, contained in the transient thermal finite element equation, equation (4.16), are related to temperature gradients through Fourier's law and are given by

$$\{E^n\} = \begin{Bmatrix} \left(-k\frac{\partial \{N\}^T}{\partial x}\{T^n\}\right)\Big|_{\text{node 1}} \\ \left(-k\frac{\partial \{N\}^T}{\partial x}\{T^n\}\right)\Big|_{\text{node 2}} \\ \left(-k\frac{\partial \{N\}^T}{\partial x}\{T^n\}\right)\Big|_{\text{node 3}} \\ \left(-k\frac{\partial \{N\}^T}{\partial x}\{T^n\}\right)\Big|_{\text{node 4}} \end{Bmatrix} \tag{4.26}$$

$$\{F^n\} = \begin{Bmatrix} \left(-k\frac{\partial\{N\}^T}{\partial y}\{T^n\}\right)_{\text{node 1}} \\ \left(-k\frac{\partial\{N\}^T}{\partial y}\{T^n\}\right)_{\text{node 2}} \\ \left(-k\frac{\partial\{N\}^T}{\partial y}\{T^n\}\right)_{\text{node 3}} \\ \left(-k\frac{\partial\{N\}^T}{\partial y}\{T^n\}\right)_{\text{node 4}} \end{Bmatrix} \tag{4.27}$$

where the gradients of the interpolation functions with respect to the Cartesian coordinates are replaced by the expressions in natural coordinates given in equations (4.24 - 4.25). These vectors are a function of nodal temperatures and hence need to be updated at every time step for the transient thermal analysis. For problems involving temperature dependent conductivity, the thermal conductivity is also easily updated. The boundary surface nodal heat flux vector {q} in equation (4.16) represents the heat flux normal to the element boundary and can be replaced by any of the several different types of boundary heating conditions given in equation (2.17). The transient thermal finite element equation, equation (4.16), is solved for the nodal change in the variable, $\{\Delta U\}$, at every time step. The temperatures at the new time step, n+1, are then determined using equation (4.13).

4.2.2 Structural Analysis

The two-dimensional quasi-static structural response is governed by the equilibrium equations. By neglecting the body forces, these equations are,

$$\frac{\partial\sigma_x}{\partial x} + \frac{\partial\tau_{xy}}{\partial y} = 0 \tag{4.28}$$

$$\frac{\partial \sigma_y}{\partial y} + \frac{\partial \tau_{xy}}{\partial x} = 0 \tag{4.29}$$

where σ_x and σ_y represent normal stresses in the x- and y-coordinate directions respectively, and τ_{xy} represents shear stress. As with the thermal formulation, the Galerkin method of weighted residuals, equation (4.9), is applied to each equilibrium equation to yield

$$\int_A N_i \left(\frac{\partial \sigma_x}{\partial x} + \frac{\partial \tau_{xy}}{\partial y}\right) dA = 0 \tag{4.30}$$

$$\int_A N_i \left(\frac{\partial \sigma_y}{\partial y} + \frac{\partial \tau_{xy}}{\partial x}\right) dA = 0 \tag{4.31}$$

where N_i, i = 1 to 8 are the nodeless variable interpolation functions given in equations (2.10) and (4.7). Integration by parts is performed on each term in equations (4.30 and 4.31) to generate the element boundary integrals yielding the equations

$$\int_A \left(\sigma_x \frac{\partial N_j}{\partial x} + \tau_{xy} \frac{\partial N_j}{\partial y}\right) dA = \int_S N_i \, T_x \, dS \tag{4.32}$$

$$\int_A \left(\sigma_y \frac{\partial N_j}{\partial y} + \tau_{xy} \frac{\partial N_j}{\partial x}\right) dA = \int_S N_i \, T_y \, dS \tag{4.33}$$

where T_x and T_y are surface tractions on the element boundaries in the x- and y-coordinate directions, respectively. Equations (4.32 - 4.33) are combined to yield sixteen equations for evaluation of the sixteen degrees of freedom of the

displacement components for the two-dimensional nodeless variable structural element. The combined representation is written in the form

$$\int_A [B_s]^T \{\sigma\}\, dA = \int_S [N]^T \{T_s\}\, dS \tag{4.34}$$

where the subscript s denotes the structural form of the matrices. The matrix $[N]^T$ is the transpose of the combined interpolation function matrix defined in equation (4.5). The matrix, $[B_s]^T$, is given by

$$[B_s]^T = \begin{bmatrix} \frac{\partial N_1}{\partial x} & 0 & \frac{\partial N_1}{\partial y} \\ 0 & \frac{\partial N_1}{\partial y} & \frac{\partial N_1}{\partial x} \\ \cdot & \cdot & \cdot \\ \cdot & \cdot & \cdot \\ \cdot & \cdot & \cdot \\ \frac{\partial N_8}{\partial x} & 0 & \frac{\partial N_8}{\partial y} \\ 0 & \frac{\partial N_8}{\partial y} & \frac{\partial N_8}{\partial x} \end{bmatrix} \tag{4.35}$$

and the vectors $\{\sigma\}$ and $\{T_s\}$ contain the stress components and surface tractions, respectively. These matrices are defined by

$$\{\sigma\} = \begin{Bmatrix} \sigma_x \\ \sigma_y \\ \tau_{xy} \end{Bmatrix} = \{\sigma_1\} - \{\sigma_2\} \tag{4.36}$$

$$\{T_s\} = \begin{Bmatrix} T_x \\ T_y \end{Bmatrix} \tag{4.37}$$

where $\{\sigma_1\}$ and $\{\sigma_2\}$ are the two-dimensional components of the stress vector associated with the displacement gradients and the temperature, respectively. The first component vector is related to the displacement gradient through the generalized Hooke's law in the form

$$\{\sigma_1\} = [C]\{\varepsilon\}$$

where

$$\{\varepsilon\} = \begin{Bmatrix} \dfrac{\partial u}{\partial x} \\ \dfrac{\partial v}{\partial y} \\ \dfrac{\partial u}{\partial y} + \dfrac{\partial v}{\partial x} \end{Bmatrix} \tag{4.38}$$

[C] is the matrix of material elastic constants and $\{\varepsilon\}$ is the vector of strain components. The second stress component vector is related to the temperature given by

$$\{\sigma_2\} = [C]\{\alpha\}(T(x,y) - T_o) \tag{4.39}$$

where $\{\alpha\}$ is the vector of thermal expansion parameters, T(x,y) is the element temperature distribution, and T_o is the reference temperature for a zero stress state. The matrix [C] and vector $\{\alpha\}$ are dependent on whether the problem being analyzed assumes a state of plane stress or plane strain. For the plane stress problem and an isotropic material, [C] and $\{\alpha\}$ are defined by

$$[C] = \frac{E}{1-\nu^2}\begin{bmatrix} 1 & \nu & 0 \\ \nu & 1 & 0 \\ 0 & 0 & \frac{1-\nu}{2} \end{bmatrix} \quad \text{and} \quad \{\alpha\} = \begin{Bmatrix} \alpha \\ \alpha \\ 0 \end{Bmatrix} \tag{4.40}$$

and for the plane strain problem [C] and {α} are defined by

$$[C] = \frac{E}{(1+\nu)(1-2\nu)}\begin{bmatrix} 1-\nu & \nu & 0 \\ \nu & 1-\nu & 0 \\ 0 & 0 & \frac{1-2\nu}{2} \end{bmatrix} \quad \text{and} \quad \{\alpha\} = \begin{Bmatrix} \alpha(1+\nu) \\ \alpha(1+\nu) \\ 0 \end{Bmatrix} \tag{4.41}$$

where E is the modulus of elasticity, ν is Poisson's ratio, and α is the coefficient of thermal expansion. Substituting equation (4.36) into equation (4.34) yields

$$\int_A [B_S]^T \{\sigma_1\}\, dA + \int_A [B_S]^T \{\sigma_2\}\, dA = \int_S [N_S]^T \{T_S\}\, dS \tag{4.42}$$

The finite element approximations are needed to discretize equation (4.42) in space. For the structural formulation, the flux-based assumptions discretize the element stresses in the same form as the displacement discretization given in equations (4.2 - 4.3). It follows from the one-dimensional formulation that the first stress component, $\{\sigma_1\}$, reduces to the bilinear approximation. The second stress component, $\{\sigma_2\}$, is directly related to temperature which is quadratic. Hence, the flux-based assumptions are defined by

$$\{\sigma_1\} = [N_1]\{\overline{\sigma_1}\} \tag{4.43}$$

where

$$[N_1] = \begin{bmatrix} \{\overline{N}\}^T & \{\overline{0}\}^T & \{\overline{0}\}^T \\ \{\overline{0}\}^T & \{\overline{N}\}^T & \{\overline{0}\}^T \\ \{\overline{0}\}^T & \{\overline{0}\}^T & \{\overline{N}\}^T \end{bmatrix}$$

and

$$\{\overline{\sigma_1}\} = \begin{Bmatrix} (\{\overline{\sigma_{1x}}\}_{i=1,4}) \\ (\{\overline{\sigma_{1y}}\}_{i=1,4}) \\ (\{\overline{\sigma_{1xy}}\}_{i=1,4}) \end{Bmatrix}$$

$$\{\sigma_2\} = [N_2]\{\overline{\sigma_2}\} \qquad (4.44)$$

where

$$[N_2] = \begin{bmatrix} \{N\}^T & \{0\}^T \\ \{0\}^T & \{N\}^T \\ \{0\}^T & \{0\}^T \end{bmatrix}$$

and

$$\{\overline{\sigma_2}\} = \begin{Bmatrix} (\{\overline{\sigma_{2x}}\}_{i=1,8}) \\ (\{\overline{\sigma_{2y}}\}_{i=1,8}) \\ \{0\} \end{Bmatrix}$$

The vectors $\{\overline{0}\}$ and $\{0\}$ are null vectors. The transpose of the vectors is given by

$$\{\overline{0}\}^T = [0\,0\,0\,0]$$

$$\{0\}^T = [0\,0\,0\,0\,0\,0\,0\,0] \tag{4.45}$$

For $\{\overline{\sigma_1}\}$, i = 1 to 4 yields the values of the first stress components evaluated at node i. For $\{\overline{\sigma_2}\}$, i = 1 to 8 yields the values of the second stress components with respect to nodes i = 1 to 4 and the nodeless variables, i = 5 to 8. The terms in $\{\overline{\sigma_1}\}$ are related to displacement gradients using equation (4.38) and the finite element approximation of the displacements, equations (4.2 - 4.3). The terms in $\{\overline{\sigma_2}\}$ are related to the temperatures using equation (4.39) and the finite element approximation of the temperature distribution, equation (4.1).

The two-dimensional hierarchical flux-based finite element equation is written in the form

$$[D_1]\{\overline{\sigma_1}\} = [D_2]\{\overline{\sigma_2}\} - [B]\{T_s\} \tag{4.46}$$

where the matrices $[D_1]$, $[D_2]$, and $[B]$ are defined by

$$[D_1] = \int_A [B_s]^T [N_1]\, dA \tag{4.47}$$

$$[D_2] = \int_A [B_s]^T [N_2]\, dA \tag{4.48}$$

$$[B] = \int_S [N]^T\, dS \tag{4.49}$$

The surface traction vector, $\{T_s\}$, is assumed here to be constant over the element surface. Transformation to natural coordinates is required for

evaluation of these matrices. As with the thermal matrices, terms in the matrix $[B_S]^T$ defined in equation (4.35) are replaced by the corresponding gradients in natural coordinates given in equations (4.24 - 4.25). Also, using the relationship $dA = |J|d\zeta d\eta$ allows for evaluation of the finite element matrices for the two-dimensional hierarchical flux-based finite element equation. To evaluate the finite element equation in terms of the unknown displacements, the vector $\{ \overline{\sigma_1} \}$ is expressed in terms of the displacement vector which can be defined as

$$\{ \overline{\sigma_1} \} = [P] \{\delta\} \tag{4.50}$$

The closed-form expressions for the terms in the two-dimensional structural finite element matrices, $[D_1]$, $[D_2]$, $[B]$, and $[P]$ and the vector $\{ \overline{\sigma_2} \}$ are given in Appendix B. Replacing $\{ \overline{\sigma_1} \}$ in equation (4.46) by the relationship given in equation (4.50), the finite element equation is evaluated in terms of $\{\delta\}$, the vector of unknown nodal displacements and nodeless variables. The values of $\{\delta\}$ are then used to evaluate the element stresses using equation (4.36) and equations (4.38 and 4.39).

4.3 Applications of Two-Dimensional Methodologies

To evaluate the two-dimensional nodeless variable flux-based method, two example problems are presented. Both example problems are for a plane stress analysis of a copper plate. The first problem is a plate with a linear temperature distribution. An exact solution for the displacement distributions is available for this problem, providing a means for verifying the accuracy of the nodeless variable flux-based solution. The second problem analyzed is for a

plate with a linear distribution of an applied heat flux over one of the plate boundaries. Solutions for both of the example problems are compared with solutions obtained using the conventional finite element method.

A schematic of the structural finite element model for the first problem analyzed is shown in figure 12(a). The copper plate is 10 in. long in the x-direction and 5 in. wide in the y-direction. A reference temperature for zero thermal stress, $T_o = 0$, was assumed. The plate is free to expand and is constrained to prevent rigid body motion. The temperature distribution within the plate was assumed to be a linear function of x, where $T(x) = 10x$, as shown in figure 12(b). Because the plate is subjected to a linear temperature distribution and is free to expand, there is no thermal stress. The exact displacement distributions are given by

$$u(x,y) = 5\,\alpha\,(x^2 - y^2) \tag{4.51}$$

$$v(x,y) = 10\,\alpha\,xy \tag{4.52}$$

where α is the coefficient of thermal expansion for copper. The exact u-displacement distributions at $y = 0$ and at $y = 5$ in. are plotted in figures 13(a) and 13(b), respectively. Also shown in figure 13(a) and 13(b) are the displacement distributions obtained from the nodeless variable flux-based and conventional methods. As can be seen from figure 13(a) and 13(b), one nodeless variable flux-based element yields the exact displacement distributions, whereas one conventional element was insufficient to accurately describe the u-displacement distributions. As shown in figure 13(a) and 13(b), four conventional elements were required to closely represent the exact solution.

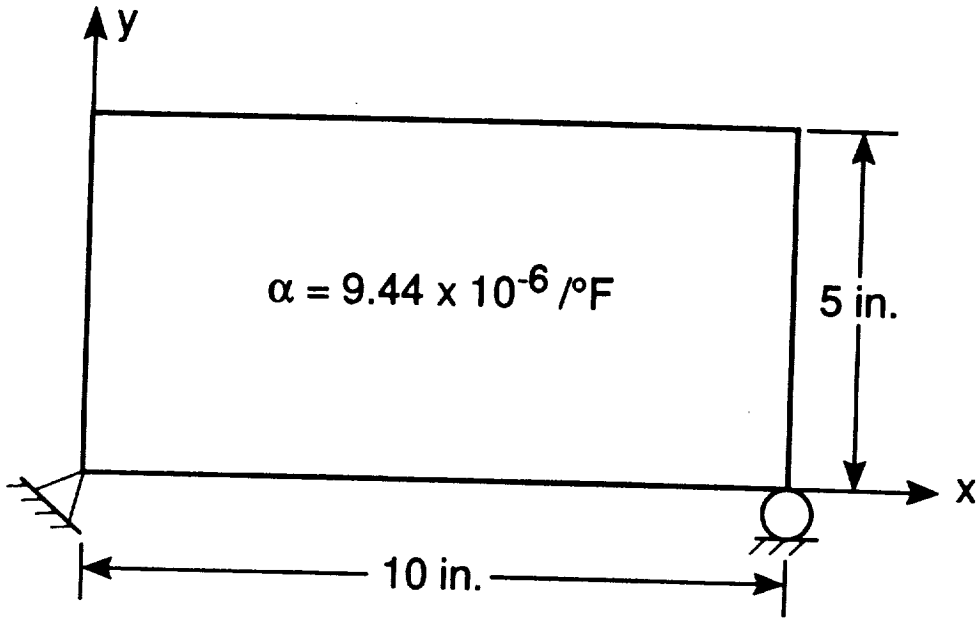

(a) Schematic diagram of structural finite element model

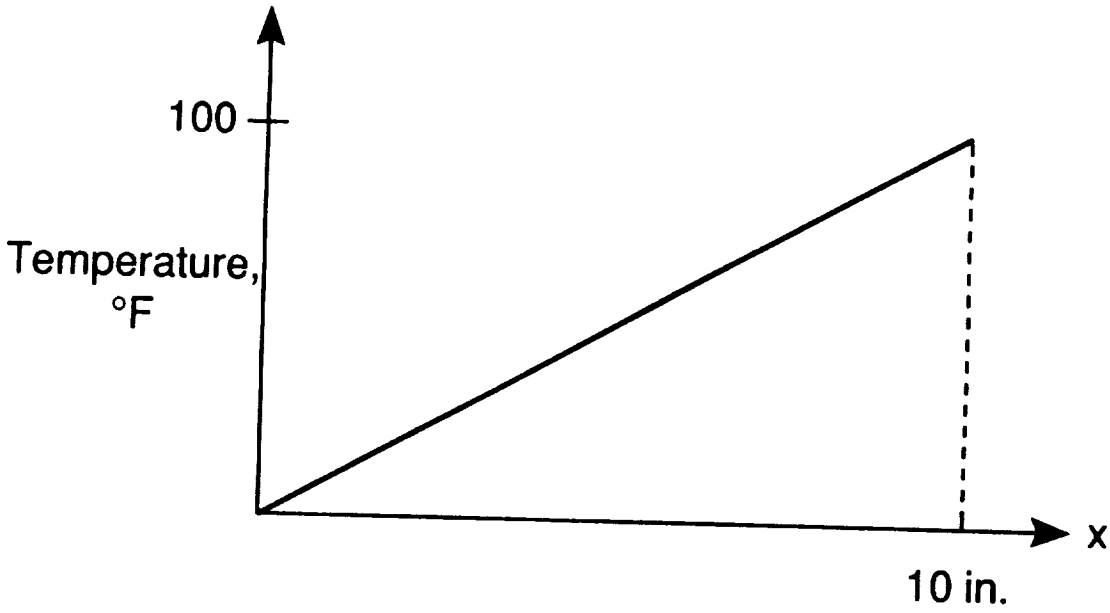

(b) Assumed temperature distribution in structural finite element model

Figure 12. Schematic diagram of structural finite element model and assumed temperature distribution.

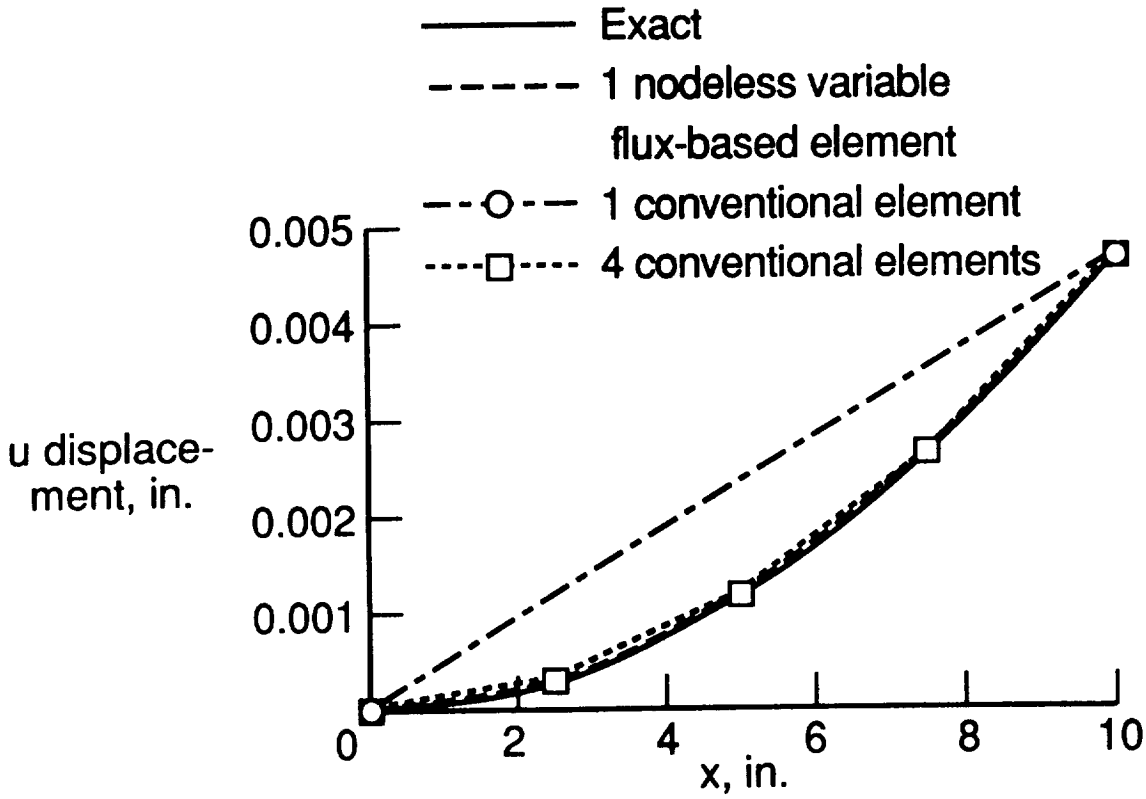

(a) u displacement distribution at y = 0

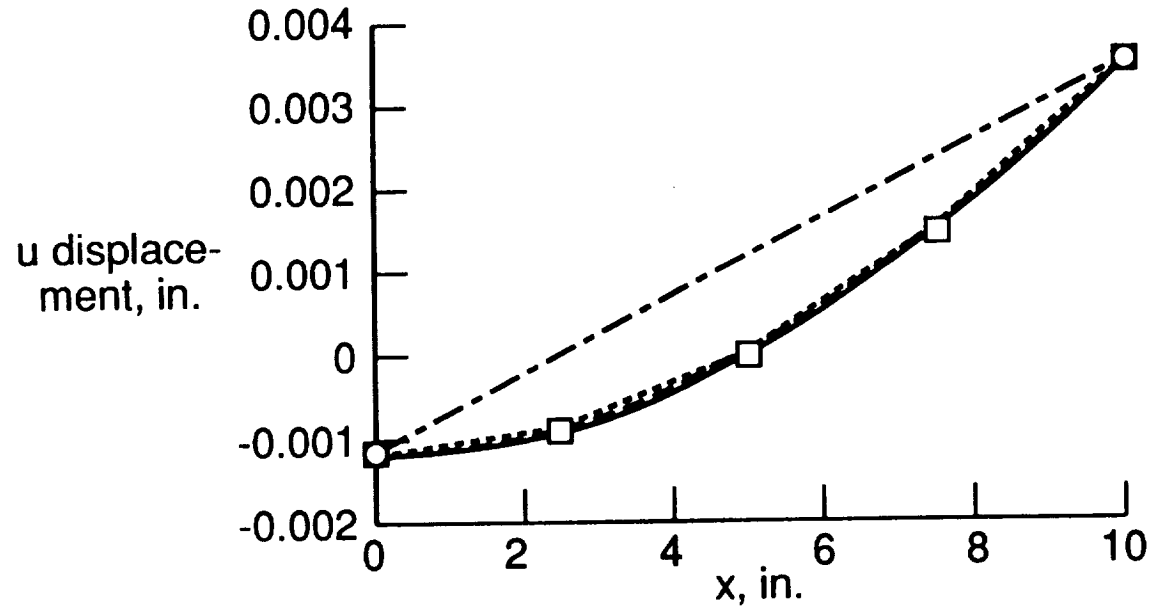

(b) u displacement distribution at y = 5 in.

Figure 13. Displacement distributions in a copper plate subjected to a linear temperature distribution.

The second problem analyzed consisted of thermal and structural analyses of a 4 in. square copper plate. The schematic diagram of the thermal and structural finite element models are shown in figures 14(a) and 14(b), respectively. For the thermal analysis, an initial temperature of $T_i = 70\ ^oF$ is assumed, where the boundary conditions consist of: (1) an applied linearly distributed heating rate, q, at x = 4 in., as shown in figure 14(a); (2) a prescribed temperature of 70^o F at y = 4 in.; (3) insulated at y = 0; and (4) insulated at x = 0. The temperature distributions along the boundaries y = 0 and x = 4 in., obtained using the nodeless variable flux-based and conventional methods are shown in figure 15(a) and 15(b) for the time t = 5 sec. The solution for the 16 x 16 mesh of conventional elements is considered to be the reference solution. A 4 x 4 mesh of nodeless variable flux-based elements is required to obtain an accurate representation of the reference solution. The temperature distributions at t = 5 sec., obtained using the 16 x 16 mesh of conventional elements and 4 x 4 mesh of nodeless variable elements, are used as the thermal loading in the structural analysis. The thermal finite element model discretizations used to obtain the temperature distributions were also used as the structural finite element model discretizations. A reference temperature for zero thermal stress, $T_o = 70\ ^oF$ is assumed. As shown in figure 14(b), the structural model is constrained from displacement in the y-coordinate direction along the boundary y = 0, and constrained from displacement in the x-coordinate direction at the corner x = y = 0. The displacement distributions were obtained using the nodeless variable flux-based method, with the 4 x 4 finite element model discretization required to accurately represent the reference temperature distribution. The displacement distributions were also obtained by using the conventional method, with the 16 x 16 finite element model discretization. The maximum displacements and

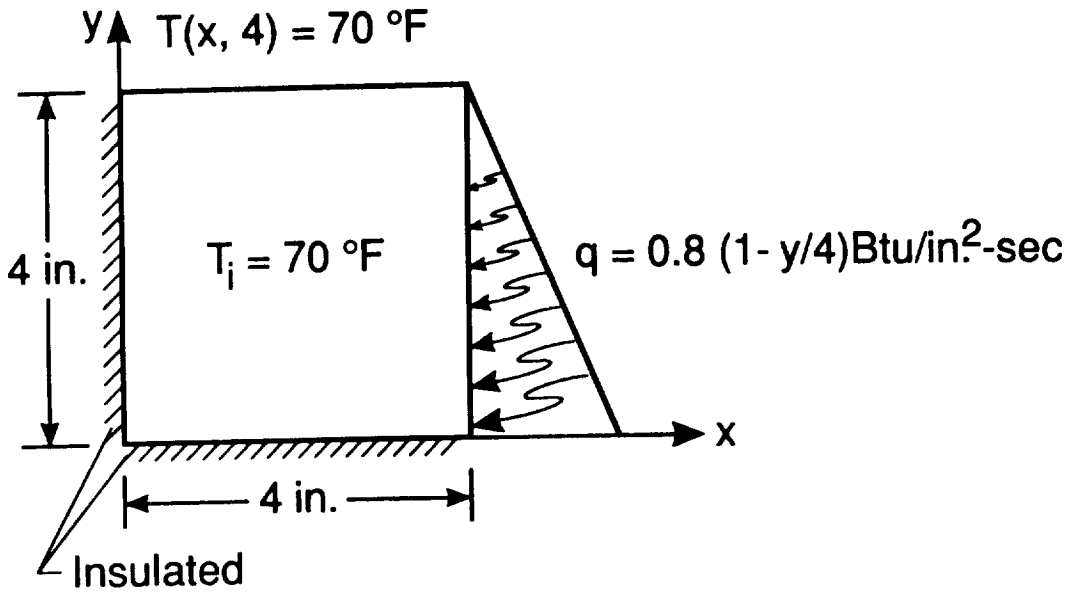

(a) Schematic diagram of thermal model

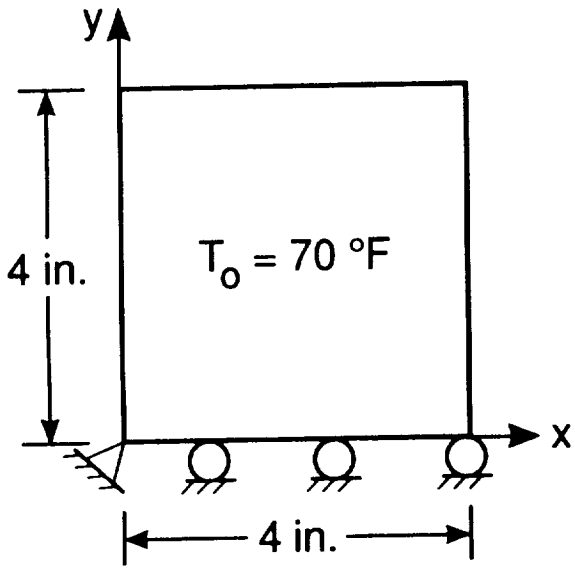

(b) Schematic diagram of structural model

Figure 14. Schematic diagram of thermal and structural finite element model of a copper plate.

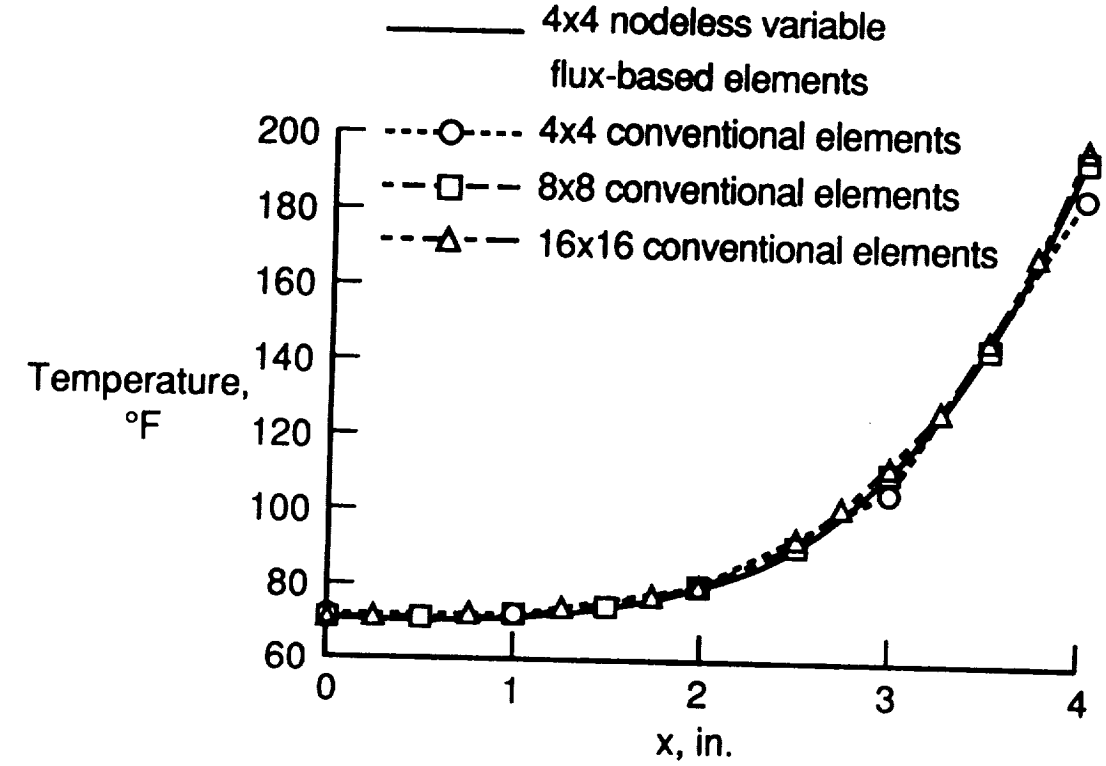

(a) Temperature distributions at y = 0

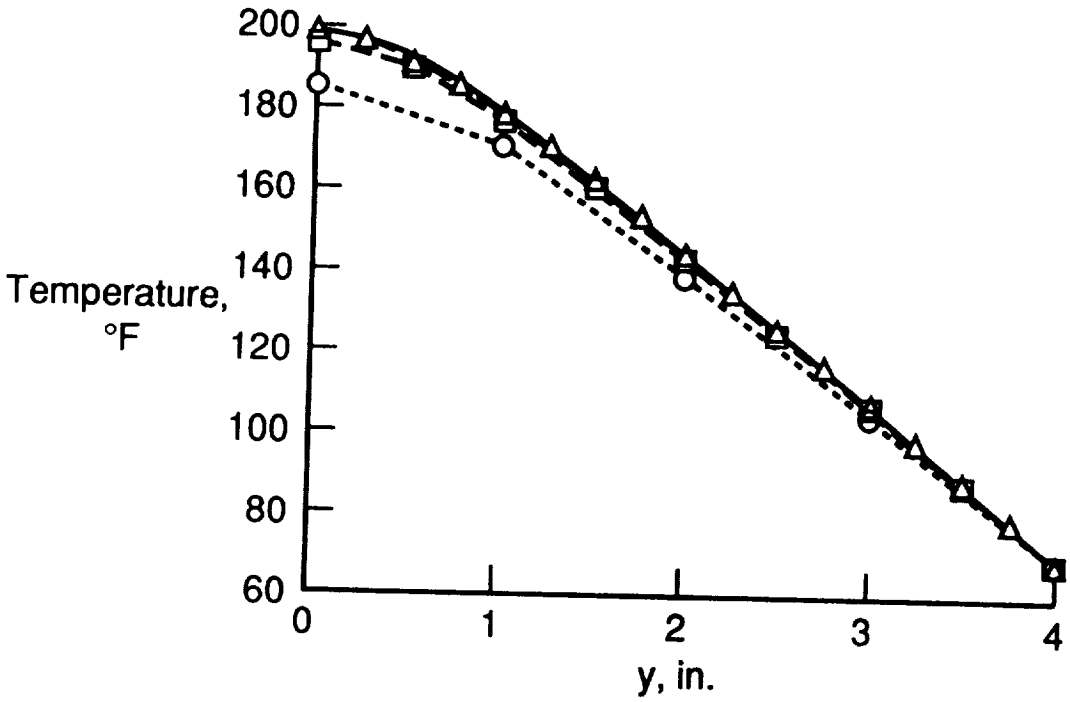

(b) Temperature distributions at x = 4 in.

Figure 15. Temperature distributions in a copper plate at t = 5 sec.

displacement gradients were observed along the boundary at x = 4 in. for the v displacement. The v displacements along the boundary at x = 4 in. obtained using the nodeless variable flux-based and conventional method are shown in figure 16(a). The maximum stress occurred along the boundary at y = 0 and normal to the y-coordinate. The average nodal stress distributions along the boundary where y = 0 obtained using the flux-based and conventional method are show in figure 16(b). Although only 4 x 4 nodeless variable elements were required to represent accurately the reference temperature and displacement distributions, a mesh of 8 x 8 nodeless variable elements is required to represent accurately the stress distribution.

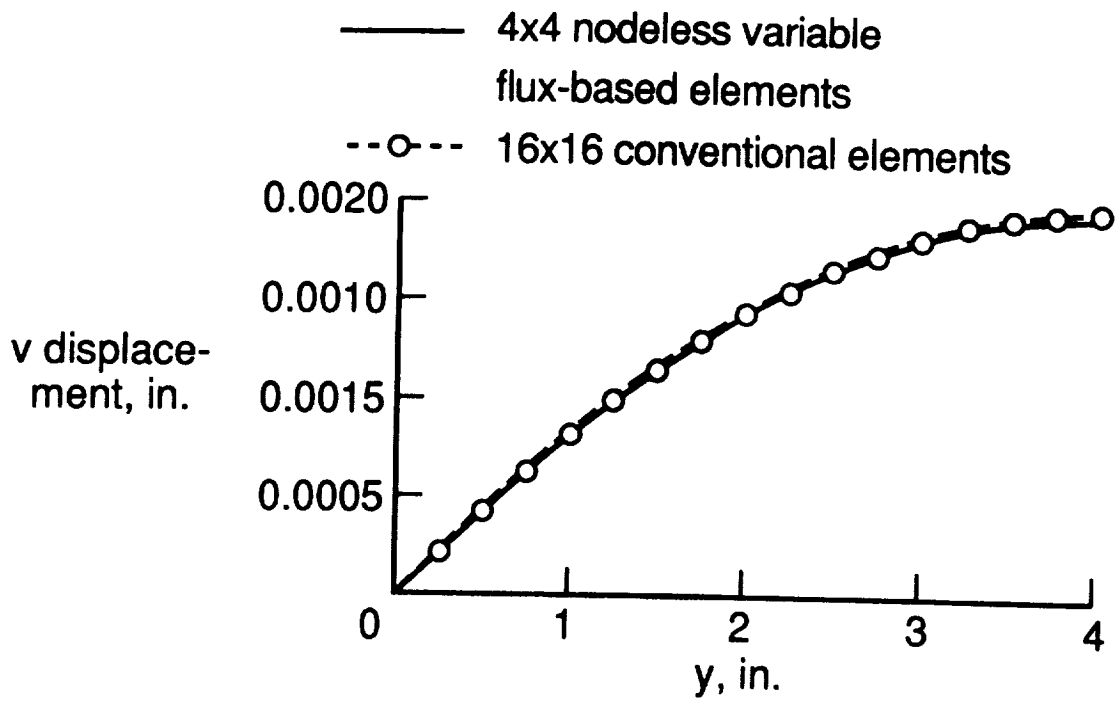

(a) v displacement distributions at x = 4 in.

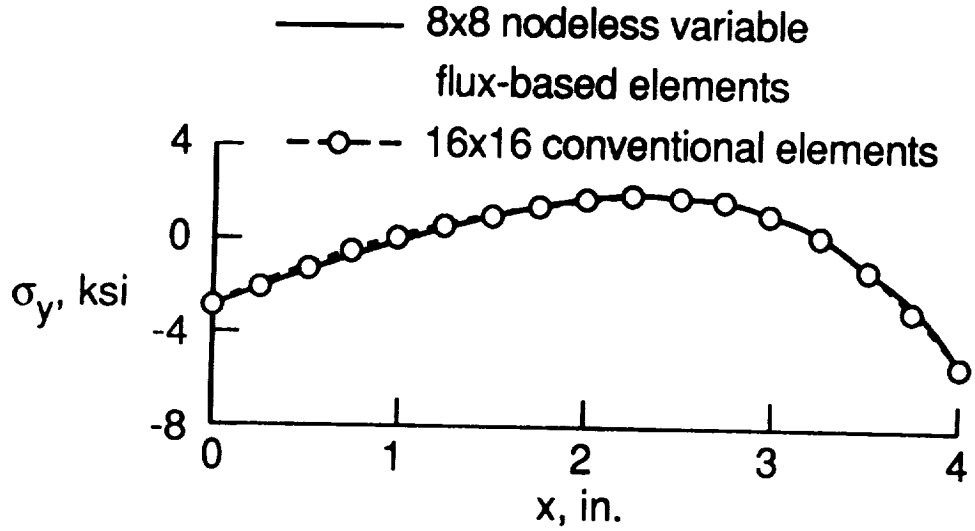

(b) Normal stress distribution in y-coordinate direction at y = 0

Figure 16. Displacement and stress distributions in a copper plate at t = 5 sec.

Chapter 5
CONCLUDING REMARKS

A hierarchical finite element method using a flux-based formulation technique is developed for both one-dimensional and two-dimensional thermal-structural analyses. The derivation of the finite element equations is presented along with the resulting finite element matrices. The finite element matrices associated with the flux-based method can be evaluated in closed-form which distinguishes the flux-based method from the conventional finite element formulation which requires numerical integration for evaluation of the finite element matrices. The hierarchical element is established by introducing additional degrees of freedom into the assumed distribution of the unknown variables by the use of nodeless variables. Employing hierarchical finite elements provides improved solution accuracy without reconstructing new finite element models. The technique also allows a single finite element model to be used for both the thermal and structural analyses, thus eliminating the difficulty in transferring data between the analyses.

Several thermal and structural example problems are analyzed to investigate the ability of the hierarchical flux-based method for predicting accurate thermal and structural responses. The resulting solutions obtained by using the hierarchical flux-based method are compared with solutions obtained using the conventional finite element method and the exact solution when available. From the resulting transient thermal solutions, the hierarchical flux-based method demonstrates an ability to provide more accurate temperature distribution results using fewer elements than the conventional finite element

method, especially when large temperature gradients are present in the structure. With the quasi-static assumption, the temperature distribution results at a specified time can be used as thermal loading in a structural analysis. To implement a temperature solution, the corresponding structural model needs to have the same discretization as the thermal model. Hence, the conventional method usually requires a structural model with more elements then the hierarchical flux-based method requires to provide an accurate temperature distribution. The hierarchical flux-based finite element method also produced accurate structural displacements and stresses using fewer elements than required by the conventional method. In general, the hierarchical flux-based elements show some improvements in accuracy for predicting thermal and structural responses as compared to using an equivalent number of conventional elements.

The hierarchical flux-based method is presently devoloped for the analysis of one- and two-dimensional membrane structures. The method is general and could be extended to three-dimensional thermal and structural analysis capabilities and developed for plate bending problems.

REFERENCES

1. Turner, M.J.; Clough, R. W.; Martin, H. C.; and Topp, L. J.: Stiffness and Deflection Analysis of Complex Structures. Journal of Aerospace Science, Vol. 23, July 1956, pp. 805-823.

2. Heubner, K.H.; and Thornton, E. A.: The Finite Element Method For Engineers. Wiley, New York, 1982.

3. Dechaumphai, P.; and Thornton, E. A.: Improved Finite Element Methodology for Integrated Thermal Structural Analysis. NASA-CR-3635, November 1982.

4. Dechaumphai, P.; and Thornton, E. A.: A Hierarchical Finite Element Approach for Integrated Thermal-Structural Analysis. AIAA 25th Structural Dynamics and Materials Conference, Palm Springs, California, AIAA Paper No. 84-0939, May 1984.

5. Thornton, E. A.; and Dechamphai, P.: Integrated Finite Element Thermal-Structural Analysis with Radiation Heat Transfer. AIAA 23th Structural Dynamics and Materials Conference, New Orleans, Louisiana, AIAA Paper No. 82-0703, May 1982.

6. Donea, J.: A Taylor-Galerkin Method for Convective Transport Problems. Numerical Methods in Thermal Problems, edited by R. W. Lewis, J. A. Johnson

and W. R. Smith, Proceedings of Third International Conference, Seattle, WA, Pineridge Press, Swansea, U. K, August 1983.

7. Donea, J.: Taylor-Galerkin Method for Convective Transport Problems. International Journal of Numerical Methods, Vol. 20, 1984, pp. 101-120.

8. Lohner, R.; Morgan, K.; and Zienkiewicz, O. C.: The Solution of Non-Linear Hyperbolic Equation Systems by the Finite Element Method. International Journal of Numerical Methods for Fluids, Vol. 4, 1984, pp. 1043-1063.

9. Lohner, R.; Morgan, K.; and Zienkiewicz, O. C.: The Use of Domain Splitting With an Explicit Hyperbolic Solver. Computational Methods in Applied Mechanical Engineering, Vol. 45, 1984, pp. 313-329.

10. Bey, K. S.; Thornton, E. A.; Dechamphai, P.; and Ramakrishnan, R.: A New Finite Element Approach for Prediction of Aerothermal Loads-Progress in Invicid Flow Computations. Proceedings of the 7th AIAA Computational Fluid Dynamics Conference, Cincinnati, OH, July 1985.

11. Thornton, E.A.; Ramakrishnan, R.; and Dechamphai, P.: A Finite Element Approach for Solution of the 3D Euler Equations. 24th Aerospace Science Meeting, Reno, Nevada, AIAA Paper No. 86-0106, January 1986.

12. Thornton, E. A.; and Dechamphai, P.: A Taylor-Galerkin Finite Element Algorithm for Transient Nonlinear Thermal-Structural Analysis. Structures, Structural Dynamics and Materials Conference, San Antonio, Texas, AIAA Paper No. 86-0911, May 1986.

13. Thornton, E. A.; and Dechamphai, P.: Finite Element Prediction of Aerothermal-Structural Interaction of Aerodynamically Heated Panels. 22nd Theromphysics Conference, Honolulu, Hawaii, AIAA Paper No. 87-1610, June 1987.

14. Dechamphai, P.; Thornton, E. A.; and Weiting, A. R.: Flow-Thermal-Structural Study of Aerodynamically Heating Leading Edges. Journal of Spacecraft and Rockets, Vol. 26, No. 4, July 1989, pp. 201-209.

15. Pandey, A. K.; Dechamphai, P.; and Weiting, A. R.: Thermal-Structural Finite Element Analysis Using Linear Flux Formulation. AIAA/ASME/ASCE/AMS/ASC 30th Structures, Structural Dynamics and Materials Conference, AIAA Paper No. 89-1224-CP, April 1989.

16. Polesky, S. P.; Dechamphai, P.; Glass, C. E.; and Pandey, A. K.: Three-Dimensional Thermal-Structural Analysis of a Swept Cowl Leading Edge Subjected to Skewed Shock-Shock Interference Heating. Journal of Thermophysics and Heat Transfer, Vol. 6, No. 1, January 1992, pp. 48-54.

17. Namburu, R.; Tamma, K.: Applicability/ Evaluation of Flux Based Representations for Linear/ Higher Order Elements for Heat Transfer in Structures: Generalized γ_T - Family. 29th Aerospace Sciences Meeting, Reno, Nevada, AIAA Paper No. 91-0159, January 1991.

18. Whetstone, W. D.: EISI-EAL Engineering Analysis Language Reference Manual. Engineering Information Systems, July 1983.

19. The Mathlab Group: MACSYMA Reference Manual. The Mathlab Group Laboratory for Computer Science, MIT, Version 9, Second Printing, December 1977.

20. Carslaw, H. S.; and Jaeger, J. C. : Conduction of Heat in Solids. Second Edition, Oxford University Press, 1959.

21. Wolfram, S.: Mathematica. Addison-Wesley Publishing Company, Inc., 1988.

Appendix A

Closed-Form Matrices for One-Dimensional Nodeless Variable Flux-Based Finite Element

The closed-form expressions for the terms in the one-dimensional nodeless variable flux-based finite element matrices used in the thermal formulation, [M] and [D] are given by

$$
\begin{aligned}
&M(1,1) = M(2,2) = L/3 \\
&M(1,2) = M(2,1) = L/6 \\
&M(1,3) = M(2,3) = M(3,1) = M(3,2) = L/12 \\
&M(3,3) = L/30
\end{aligned}
\tag{A.1}
$$

$$
\begin{aligned}
&D(1,1) = D(1,2) = -1/2 \\
&D(2,1) = D(2,2) = 1/2 \\
&D(3,1) = 1/6 \\
&D(3,2) = -1/6
\end{aligned}
\tag{A.2}
$$

For the structural formulation, the matrix $[D_2]$ and the matrix [P] are given by

$$
\begin{aligned}
&D_2(1,1) = D_2(1,2) = -1/2 \\
&D_2(2,1) = D_2(2,2) = 1/2 \\
&D_2(3,1) = 1/6 \\
&D_2(1,3) = -1/6 \\
&D_2(2,3) = 1/6 \\
&D_2(3,2) = -1/6 \\
&D_2(1,3) = -1/6 \\
&D_2(2,3) = 1/6 \\
&D_2(3,3) = 0
\end{aligned}
\tag{A.3}
$$

$$P(1,1) = P(2,2) = E/L$$
$$P(1,2) = P(2,1) = -E/L$$
$$P(1,3) = P(2,3) = P(3,1) = P(3,2) = 0$$
$$P(3,3) = E/3L \qquad \text{(A.4)}$$

Appendix B

Closed-Form Matrices for Two-Dimensional Nodeless Variable Flux-Based Finite Element

The determinant of the Jacobian matrix, $|J|$, is required for evaluation of the two-dimensional finite element matrices. It can be expressed in a simplified form as

$$|J| = \sum_{i=1}^{4} N_i(\zeta,\eta)\, v_i \tag{B.1}$$

where N_i, i = 1 to 4 are the linear element interpolation functions. The terms v_i are defined by

$$\begin{aligned} v_1 &= ((x_2-x_1)(y_4-y_1)-(x_4-x_1)(y_2-y_1))/4 \\ v_2 &= ((x_2-x_1)(y_3-y_2)-(x_3-x_2)(y_2-y_1))/4 \\ v_3 &= ((x_3-x_2)(y_4-y_3)-(x_4-x_3)(y_3-y_2))/4 \\ v_4 &= ((x_4-x_1)(y_4-y_3)-(x_4-x_3)(y_4-y_1))/4 \end{aligned} \tag{B.2}$$

where x_i and y_i, i = 1 to 4 are the x- and y-coordinates of node i. The coefficients in the thermal finite element mass matrix are evaluated using the expression

$$M(i,j) = \int_{-1}^{1}\int_{-1}^{1} N_i N_j \left(\sum_{k=1}^{4} N_k v_k\right) d\zeta\, d\eta \tag{B.3}$$

where each coefficient is evaluated as

$$M(1,1) = (9v_1 + 3v_2 + v_3 + 3v_4)/36$$

$$M(1,2) = (3v_1 + 3v_2 + v_3 + v_4)/36$$
$$M(1,3) = (v_1 + v_2 + v_3 + v_4)/36$$
$$M(1,4) = (3v_1 + v_2 + v_3 + 3v_4)/36$$
$$M(1,5) = (9v_1 + 6v_2 + 2v_3 + 3v_4)/180$$
$$M(1,6) = (3v_1 + 3v_2 + 2v_3 + 2v_4)/180$$
$$M(1,7) = (3v_1 + 2v_2 + 2v_3 + 3v_4)/180$$
$$M(1,8) = (9v_1 + 3v_2 + 2v_3 + 6v_4)/180$$
$$M(2,1) = (3v_1 + 3v_2 + v_3 + v_4)/36$$
$$M(2,2) = (3v_1 + 9v_2 + 3v_3 + v_4)/36$$
$$M(2,3) = (v_1 + 3v_2 + 3v_3 + v_4)/36$$
$$M(2,4) = (v_1 + v_2 + v_3 + v_4)/36$$
$$M(2,5) = (6v_1 + 9v_2 + 3v_3 + 2v_4)/180$$
$$M(2,6) = (3v_1 + 9v_2 + 6v_3 + 2v_4)/180$$
$$M(2,7) = (2v_1 + 3v_2 + 3v_3 + 2v_4)/180$$
$$M(2,8) = (3v_1 + 3v_2 + 2v_3 + 2v_4)/180$$
$$M(3,1) = (v_1 + v_2 + v_3 + v_4)/36$$
$$M(3,2) = (v_1 + 3v_2 + 3v_3 + v_4)/36$$
$$M(3,3) = (v_1 + 3v_2 + 9v_3 + 3v_4)/36$$
$$M(3,4) = (v_1 + v_2 + 3v_3 + 3v_4)/36$$
$$M(3,5) = (2v_1 + 3v_2 + 3v_3 + 2v_4)/180$$
$$M(3,6) = (2v_1 + 6v_2 + 9v_3 + 3v_4)/180$$
$$M(3,7) = (2v_1 + 3v_2 + 9v_3 + 6v_4)/180$$
$$M(3,8) = (2v_1 + 2v_2 + 3v_3 + 3v_4)/180$$
$$M(4,1) = (3v_1 + v_2 + v_3 + 3v_4)/36$$
$$M(4,2) = (v_1 + v_2 + v_3 + v_4)/36$$
$$M(4,3) = (v_1 + v_2 + 3v_3 + 3v_4)/36$$
$$M(4,4) = (3v_1 + v_2 + 3v_3 + 9v_4)/36$$
$$M(4,5) = (3v_1 + 2v_2 + 2v_3 + 3v_4)/180$$
$$M(4,6) = (2v_1 + 2v_2 + 3v_3 + 3v_4)/180$$
$$M(4,7) = (3v_1 + 2v_2 + 6v_3 + 9v_4)/180$$
$$M(4,8) = (6v_1 + 2v_2 + 3v_3 + 9v_4)/180$$
$$M(5,1) = (9v_1 + 6v_2 + 2v_3 + 3v_4)/180$$
$$M(5,2) = (6v_1 + 9v_2 + 3v_3 + 2v_4)/180$$
$$M(5,3) = (2v_1 + 3v_2 + 3v_3 + 2v_4)/180$$
$$M(5,4) = (3v_1 + 2v_2 + 2v_3 + 3v_4)/180$$
$$M(5,5) = (3v_1 + 3v_2 + v_3 + v_4)/180$$

$$
\begin{aligned}
M(5,6) &= (6v_1 + 9v_2 + 6v_3 + 4v_4)/900 \\
M(5,7) &= (v_1 + v_2 + v_3 + v_4)/180 \\
M(5,8) &= (9v_1 + 6v_2 + 4v_3 + 6v_4)/900 \\
M(6,1) &= (3v_1 + 3v_2 + 2v_3 + 2v_4)/180 \\
M(6,2) &= (3v_1 + 9v_2 + 6v_3 + 2v_4)/180 \\
M(6,3) &= (2v_1 + 6v_2 + 9v_3 + 3v_4)/180 \\
M(6,4) &= (2v_1 + 2v_2 + 3v_3 + 3v_4)/180 \\
M(6,5) &= (6v_1 + 9v_2 + 6v_3 + 4v_4)/900 \\
M(6,6) &= (v_1 + 3v_2 + 3v_3 + v_4)/180 \\
M(6,7) &= (4v_1 + 6v_2 + 9v_3 + 6v_4)/900 \\
M(6,8) &= (v_1 + v_2 + v_3 + v_4)/180 \\
M(7,1) &= (3v_1 + 2v_2 + 2v_3 + 3v_4)/180 \\
M(7,2) &= (2v_1 + 3v_2 + 3v_3 + 2v_4)/180 \\
M(7,3) &= (2v_1 + 3v_2 + 9v_3 + 6v_4)/180 \\
M(7,4) &= (3v_1 + 2v_2 + 6v_3 + 9v_4)/180 \\
M(7,5) &= (v_1 + v_2 + v_3 + v_4)/180 \\
M(7,6) &= (4v_1 + 6v_2 + 9v_3 + 6v_4)/900 \\
M(7,7) &= (v_1 + v_2 + 3v_3 + 3v_4)/180 \\
M(7,8) &= (6v_1 + 4v_2 + 6v_3 + 9v_4)/900 \\
M(8,1) &= (9v_1 + 3v_2 + 2v_3 + 6v_4)/180 \\
M(8,2) &= (3v_1 + 3v_2 + 2v_3 + 2v_4)/180 \\
M(8,3) &= (2v_1 + 2v_2 + 3v_3 + 3v_4)/180 \\
M(8,4) &= (6v_1 + 2v_2 + 3v_3 + 9v_4)/180 \\
M(8,5) &= (9v_1 + 6v_2 + 4v_3 + 6v_4)/900 \\
M(8,6) &= (v_1 + v_2 + v_3 + v_4)/180 \\
M(8,7) &= (6v_1 + 4v_2 + 6v_3 + 9v_4)/900 \\
M(8,8) &= (3v_1 + v_2 + v_3 + 3v_4)/180
\end{aligned}
\tag{B.4}
$$

The coefficients in the thermal finite element matrices, $[D_x]$ and $[D_y]$, are evaluated using the expressions

$$
D_x(i,j) = \int_{-1}^{1} \int_{-1}^{1} \left(J_{22} \frac{\partial N_i}{\partial \zeta} - J_{12} \frac{\partial N_i}{\partial \eta} \right) \{ \overline{N} \}^T \, d\zeta \, d\eta \tag{B.5}
$$

$$D_y(i,j) = \int_{-1}^{1}\int_{-1}^{1}\left(-J_{21}\frac{\partial N_i}{\partial \zeta} + J_{11}\frac{\partial N_j}{\partial \eta}\right)\{\overline{N}\}^T d\zeta\, d\eta \qquad \text{(B.6)}$$

where each coefficient in $D_x(i,j)$ is evaluated as

$$D_x(1,1) = (y_2 - y_4)/6$$
$$D_x(1,2) = (2y_2 - y_3 - y_4)/12$$
$$D_x(1,3) = (y_2 - y_4)/12$$
$$D_x(1,4) = (y_2 + y_3 - 2y_4)/12$$
$$D_x(2,1) = (-2y_1 + y_3 + y_4)/12$$
$$D_x(2,2) = (-y_1 + y_3)/6$$
$$D_x(2,3) = (-y_1 + 2y_3 - y_4)/12$$
$$D_x(2,4) = (-y_1 + y_3)/12$$
$$D_x(3,1) = (-y_2 + y_4)/12$$
$$D_x(3,2) = (y_1 - 2y_2 + y_4)/12$$
$$D_x(3,3) = (-y_2 + y_4)/6$$
$$D_x(3,4) = (-y_1 - y_2 + 2y_4)/12$$
$$D_x(4,1) = (2y_1 - y_2 - y_3)/12$$
$$D_x(4,2) = (y_1 - y_3)/12$$
$$D_x(4,3) = (y_1 + y_2 - 2y_3)/12$$
$$D_x(4,4) = (y_1 - y_3)/6$$
$$D_x(5,1) = (-6y_1 + 2y_2 + y_3 + 3y_4)/72$$
$$D_x(5,2) = (-2y_1 + 6y_2 - 3y_3 - y_4)/72$$
$$D_x(5,3) = (-y_1 + 3y_2 - 2y_4)/72$$
$$D_x(5,4) = (-3y_1 + y_2 + 2y_3)/72$$
$$D_x(6,1) = (-3y_2 + y_3 + 2y_4)/72$$
$$D_x(6,2) = (3y_1 - 6y_2 + 2y_3 + y_4)/72$$
$$D_x(6,3) = (-y_1 - 2y_2 + 6y_3 - 3y_4)/72$$
$$D_x(6,4) = (-2y_1 - y_2 + 3y_3)/72$$
$$D_x(7,1) = (-2y_2 - y_3 + 3y_4)/72$$
$$D_x(7,2) = (2y_1 - 3y_3 + y_4)/72$$
$$D_x(7,3) = (y_1 + 3y_2 - 6y_3 + 2y_4)/72$$
$$D_x(7,4) = (-3y_1 - y_2 - 2y_3 + 6y_4)/72$$
$$D_x(8,1) = (6y_1 - 3y_2 - y_3 - 2y_4)/72$$
$$D_x(8,2) = (3y_1 - 2y_3 - y_4)/72$$

$$D_x(8,3) = (y_1 + 2y_2 - 3y_4)/72$$
$$D_x(8,4) = (2y_1 + y_2 + 3y_3 - 6y_4)/72 \qquad \text{(B.7)}$$

and each coefficient in $D_y(i,j)$ is evaluated as

$$D_y(1,1) = (-x_2 + x_4)/6$$
$$D_y(1,2) = (-2x_2 + x_3 + x_4)/12$$
$$D_y(1,3) = (-x_2 + x_4)/12$$
$$D_y(1,4) = (-x_2 - x_3 + 2x_4)/12$$
$$D_y(2,1) = (2x_1 - x_3 - x_4)/12$$
$$D_y(2,2) = (x_1 - x_3)/6$$
$$D_y(2,3) = (x_1 - 2x_3 + x_4)/12$$
$$D_y(2,4) = (x_1 - x_3)/12$$
$$D_y(3,1) = (x_2 - x_4)/12$$
$$D_y(3,2) = (-x_1 + 2x_2 - x_4)/12$$
$$D_y(3,3) = (x_2 - x_4)/6$$
$$D_y(3,4) = (x_1 + x_2 - 2x_4)/12$$
$$D_y(4,1) = (-2x_1 + x_2 + x_3)/12$$
$$D_y(4,2) = (-x_1 + x_3)/12$$
$$D_y(4,3) = (-x_1 - x_2 + 2x_3)/12$$
$$D_y(4,4) = (-x_1 + x_3)/6$$
$$D_y(5,1) = (6x_1 - 2x_2 - x_3 - 3x_4)/72$$
$$D_y(5,2) = (2x_1 - 6x_2 + 3x_3 + x_4)/72$$
$$D_y(5,3) = (x_1 - 3x_2 + 2x_4)/72$$
$$D_y(5,4) = (3x_1 - x_2 - 2x_3)/72$$
$$D_y(6,1) = (3x_2 - x_3 - 2x_4)/72$$
$$D_y(6,2) = (-3x_1 + 6x_2 - 2x_3 - x_4)/72$$
$$D_y(6,3) = (x_1 + 2x_2 - 6x_3 + 3x_4)/72$$
$$D_y(6,4) = (2x_1 + x_2 - 3x_3)/72$$
$$D_y(7,1) = (2x_2 + x_3 - 3x_4)/72$$
$$D_y(7,2) = (-2x_1 + 3x_3 - x_4)/72$$
$$D_y(7,3) = (-x_1 - 3x_2 + 6x_3 - 2x_4)/72$$
$$D_y(7,4) = (3x_1 + x_2 + 2x_3 - 6x_4)/72$$
$$D_y(8,1) = (-6x_1 + 3x_2 + x_3 + 2x_4)/72$$
$$D_y(8,2) = (-3x_1 + 2x_3 + x_4)/72$$
$$D_y(8,3) = (-x_1 - 2x_2 + 3x_4)/72$$

$$D_y(8,4) = (-2x_1 - x_2 - 3x_3 + 6x_4)/72 \qquad \text{(B.8)}$$

The boundary matrix, [B], for the thermal formulation is evaluated over the element surface (i.e., the element edge) using the one-dimensional interpolation functions. The coefficients in the thermal boundary matrix are given by

$$\begin{aligned} B(1,1) &= L/3 \\ B(1,2) &= L/6 \\ B(2,1) &= L/6 \\ B(2,2) &= L/3 \\ B(3,1) &= L/12 \\ B(3,2) &= L/12 \end{aligned} \qquad \text{(B.9)}$$

where L is the length of the element edge where the applied heating is defined.

For the structural formulation, the coefficients in the finite element matrix, $[D_1]$ are given by

$$\begin{aligned} D_1(1,1) &= (y_2 - y_4)/6 \\ D_1(1,2) &= (2y_2 - y_3 - y_4)/12 \\ D_1(1,3) &= (y_2 - y_4)/12 \\ D_1(1,4) &= (y_2 + y_3 - 2y_4)/12 \\ D_1(1,5) &= 0 \\ D_1(1,6) &= 0 \\ D_1(1,7) &= 0 \\ D_1(1,8) &= 0 \\ D_1(1,9) &= (-x_2 + x_4)/6 \\ D_1(1,10) &= (-2x_2 + x_3 + x_4)/12 \\ D_1(1,11) &= (-x_2 + x_4)/12 \\ D_1(1,12) &= (-x_2 - x_3 + 2x_4)/12 \\ D_1(2,1) &= 0 \\ D_1(2,2) &= 0 \\ D_1(2,3) &= 0 \end{aligned}$$

$D_1(2,4) = 0$

$D_1(2,5) = (-x_2 + x_4)/6$

$D_1(2,6) = (-2x_2 + x_3 + x_4)/12$

$D_1(2,7) = (-x_2 + x_4)/12$

$D_1(2,8) = (-x_2 - x_3 + 2x_4)/12$

$D_1(2,9) = (y_2 - y_4)/6$

$D_1(2,10) = (2y_2 - y_3 - y_4)/12$

$D_1(2,11) = (y_2 - y_4)/12$

$D_1(2,12) = (y_2 + y_3 - 2y_4)/12$

$D_1(3,1) = (-2y_1 + y_3 + y_4)/12$

$D_1(3,2) = (-y_1 + y_3)/6$

$D_1(3,3) = (-y_1 + 2y_3 - y_4)/12$

$D_1(3,4) = (-y_1 + y_3)/12$

$D_1(3,5) = 0$

$D_1(3,6) = 0$

$D_1(3,7) = 0$

$D_1(3,8) = 0$

$D_1(3,9) = (2x_1 - x_3 - x_4)/12$

$D_1(3,10) = (x_1 - x_3)/6$

$D_1(3,11) = (x_1 - 2x_3 + x_4)/12$

$D_1(3,12) = (x_1 - x_3)/12$

$D_1(4,1) = 0$

$D_1(4,2) = 0$

$D_1(4,3) = 0$

$D_1(4,4) = 0$

$D_1(4,5) = (2x_1 - x_3 - x_4)/12$

$D_1(4,6) = (x_1 - x_3)/6$

$D_1(4,7) = (x_1 - 2x_3 + x_4)/12$

$D_1(4,8) = (x_1 - x_3)/12$

$D_1(4,9) = (-2y_1 + y_3 + y_4)/12$

$D_1(4,10) = (-y_1 + y_3)/6$

$D_1(4,11) = (-y_1 + 2y_3 - y_4)/12$

$D_1(4,12) = (-y_1 + y_3)/12$

$D_1(5,1) = (-y_2 + y_4)/12$

$D_1(5,2) = (y_1 - 2y_2 + y_4)/12$

$D_1(5,3) = (-y_2 + y_4)/6$

$D_1(5,4) = (-y_1 - y_2 + 2y_4)/12$

$D_1(5,5) = 0$

$D_1(5,6) = 0$

$D_1(5,7) = 0$

$D_1(5,8) = 0$

$D_1(5,9) = (x_2 - x_4)/12$

$D_1(5,10) = (-x_1 + 2x_2 - x_4)/12$

$D_1(5,11) = (x_2 - x_4)/6$

$D_1(5,12) = (x_1 + x_2 - 2x_4)/12$

$D_1(6,1) = 0$

$D_1(6,2) = 0$

$D_1(6,3) = 0$

$D_1(6,4) = 0$

$D_1(6,5) = (x_2 - x_4)/12$

$D_1(6,6) = (-x_1 + 2x_2 - x_4)/12$

$D_1(6,7) = (x_2 - x_4)/6$

$D_1(6,8) = (x_1 + x_2 - 2x_4)/12$

$D_1(6,9) = (-y_2 + y_4)/12$

$D_1(6,10) = (y_1 - 2y_2 + y_4)/12$

$D_1(6,11) = (-y_2 + y_4)/6$

$D_1(6,12) = (-y_1 - y_2 + 2y_4)/12$

$D_1(7,1) = (2y_1 - y_2 - y_3)/12$

$D_1(7,2) = (y_1 - y_3)/12$

$D_1(7,3) = (y_1 + y_2 - 2y_3)/12$

$D_1(7,4) = (y_1 - y_3)/6$

$D_1(7,5) = 0$

$D_1(7,6) = 0$

$D_1(7,7) = 0$

$D_1(7,8) = 0$

$D_1(7,9) = (-2x_1 + x_2 + x_3)/12$

$D_1(7,10) = (-x_1 + x_3)/12$

$D_1(7,11) = (-x_1 - x_2 + 2x_3)/12$

$D_1(7,12) = (-x_1 + x_3)/6$

$D_1(8,1) = 0$

$D_1(8,2) = 0$

$D_1(8,3) = 0$

$D_1(8,4) = 0$

$D_1(8,5) = (-2x_1 + x_2 + x_3)/12$

$D_1(8,6) = (-x_1 + x_3)/12$

$D_1(8,7) = (-x_1 - x_2 + 2x_3)/12$

$D_1(8,8) = (-x_1 + x_3)/6$

$D_1(8,9) = (2y_1 - y_2 - y_3)/12$

$D_1(8,10) = (y_1 - y_3)/12$

$D_1(8,11) = (y_1 + y_2 - 2y_3)/12$

$D_1(8,12) = (y_1 - y_3)/6$

$D_1(9,1) = (-6y_1 + 2y_2 + y_3 + 3y_4)/72$

$D_1(9,2) = (-2y_1 + 6y_2 - 3y_3 - y_4)/72$

$D_1(9,3) = (-y_1 + 3y_2 - 2y_4)/72$

$D_1(9,4) = (-3y_1 + y_2 + 2y_3)/72$

$D_1(9,5) = 0$

$D_1(9,6) = 0$

$D_1(9,7) = 0$

$D_1(9,8) = 0$

$D_1(9,9) = (6x_1 - 2x_2 - x_3 - 3x_4)/72$

$D_1(9,10) = (2x_1 - 6x_2 + 3x_3 + x_4)/72$

$D_1(9,11) = (x_1 - 3x_2 + 2x_4)/72$

$D_1(9,12) = (3x_1 - x_2 - 2x_3)/72$

$D_1(10,1) = 0$

$D_1(10,2) = 0$

$D_1(10,3) = 0$

$D_1(10,4) = 0$

$D_1(10,5) = (6x_1 - 2x_2 - x_3 - 3x_4)/72$

$D_1(10,6) = (2x_1 - 6x_2 + 3x_3 + x_4)/72$

$D_1(10,7) = (x_1 - 3x_2 + 2x_4)/72$

$D_1(10,8) = (3x_1 - x_2 - 2x_3)/72$

$D_1(10,9) = (-6y_1 + 2y_2 + y_3 + 3y_4)/72$

$D_1(10,10) = (-2y_1 + 6y_2 - 3y_3 - y_4)/72$

$D_1(10,11) = (-y_1 + 3y_2 - 2y_4)/72$

$D_1(10,12) = (-3y_1 + y_2 + 2y_3)/72$

$D_1(11,1) = (-3y_2 + y_3 + 2y_4)/72$

$D_1(11,2) = (3y_1 - 6y_2 + 2y_3 + y_4)/72$

$D_1(11,3) = (-y_1 - 2y_2 + 6y_3 - 3y_4)/72$

$D_1(11,4) = (-2y_1 - y_2 + 3y_3)/72$

$D_1(11,5) = 0$

$D_1(11,6) = 0$

$D_1(11,7) = 0$

$D_1(11,8) = 0$

$D_1(11,9) = (3x_2 - x_3 - 2x_4)/72$

$D_1(11,10) = (-3x_1 + 6x_2 - 2x_3 - x_4)/72$

$D_1(11,11) = (x_1 + 2x_2 - 6x_3 + 3x_4)/72$

$D_1(11,12) = (2x_1 + x_2 - 3x_3)/72$

$D_1(12,1) = 0$

$D_1(12,2) = 0$

$D_1(12,3) = 0$

$D_1(12,4) = 0$

$D_1(12,5) = (3x_2 - x_3 - 2x_4)/72$

$D_1(12,6) = (-3x_1 + 6x_2 - 2x_3 - x_4)/72$

$D_1(12,7) = (x_1 + 2x_2 - 6x_3 + 3x_4)/72$

$D_1(12,8) = (2x_1 + x_2 - 3x_3)/72$

$D_1(12,9) = (-3y_2 + y_3 + 2y_4)/72$

$D_1(12,10) = (3y_1 - 6y_2 + 2y_3 + y_4)/72$

$D_1(12,11) = (-y_1 - 2y_2 + 6y_3 - 3y_4)/72$

$D_1(12,12) = (-2y_1 - y_2 + 3y_3)/72$

$D_1(13,1) = (-2y_2 - y_3 + 3y_4)/72$

$D_1(13,2) = (2y_1 - 3y_3 + y_4)/72$

$D_1(13,3) = (y_1 + 3y_2 - 6y_3 + 2y_4)/72$

$D_1(13,4) = (-3y_1 - y_2 - 2y_3 + 6y_4)/72$

$D_1(13,5) = 0$

$D_1(13,6) = 0$

$D_1(13,7) = 0$

$D_1(13,8) = 0$

$D_1(13,9) = (2x_2 + x_3 - 3x_4)/72$

$D_1(13,10) = (-2x_1 + 3x_3 - x_4)/72$

$D_1(13,11) = (-x_1 - 3x_2 + 6x_3 - 2x_4)/72$

$D_1(13,12) = (3x_1 + x_2 + 2x_3 - 6x_4)/72$

$D_1(14,1) = 0$

$D_1(14,2) = 0$

$D_1(14,3) = 0$

$$
\begin{aligned}
&D_1(14,4) = 0\\
&D_1(14,5) = (2x_2 + x_3 - 3x_4)/72\\
&D_1(14,6) = (-2x_1 + 3x_3 - x_4)/72\\
&D_1(14,7) = (-x_1 - 3x_2 + 6x_3 - 2x_4)/72\\
&D_1(14,8) = (3x_1 + x_2 + 2x_3 - 6x_4)/72\\
&D_1(14,9) = (-2y_2 - y_3 + 3y_4)/72\\
&D_1(14,10) = (2y_1 - 3y_3 + y_4)/72\\
&D_1(14,11) = (y_1 + 3y_2 - 6y_3 + 2y_4)/72\\
&D_1(14,12) = (-3y_1 - y_2 - 2y_3 + 6y_4)/72\\
&D_1(15,1) = (6y_1 - 3y_2 - y_3 - 2y_4)/72\\
&D_1(15,2) = (3y_1 - 2y_3 - y_4)/72\\
&D_1(15,3) = (y_1 + 2y_2 - 3y_4)/72\\
&D_1(15,4) = (2y_1 + y_2 + 3y_3 - 6y_4)/72\\
&D_1(15,5) = 0\\
&D_1(15,6) = 0\\
&D_1(15,7) = 0\\
&D_1(15,8) = 0\\
&D_1(15,9) = (-6x_1 + 3x_2 + x_3 + 2x_4)/72\\
&D_1(15,10) = (-3x_1 + 2x_3 + x_4)/72\\
&D_1(15,11) = (-x_1 - 2x_2 + 3x_4)/72\\
&D_1(15,12) = (-2x_1 - x_2 - 3x_3 + 6x_4)/72\\
&D_1(16,1) = 0\\
&D_1(16,2) = 0\\
&D_1(16,3) = 0\\
&D_1(16,4) = 0\\
&D_1(16,5) = (-6x_1 + 3x_2 + x_3 + 2x_4)/72\\
&D_1(16,6) = (-3x_1 + 2x_3 + x_4)/72\\
&D_1(16,7) = (-x_1 - 2x_2 + 3x_4)/72\\
&D_1(16,8) = (-2x_1 - x_2 - 3x_3 + 6x_4)/72\\
&D_1(16,9) = (6y_1 - 3y_2 - y_3 - 2y_4)/72\\
&D_1(16,10) = (3y_1 - 2y_3 - y_4)/72\\
&D_1(16,11) = (y_1 + 2y_2 - 3y_4)/72\\
&D_1(16,12) = (2y_1 + y_2 + 3y_3 - 6y_4)/72
\end{aligned}
\qquad \text{(B.10)}
$$

and the coefficients in the matrix $[D_2]$ are given by

$$D_2(1,1) = (y_2 - y_4)/6$$
$$D_2(1,2) = (2y_2 - y_3 - y_4)/12$$
$$D_2(1,3) = (y_2 - y_4)/12$$
$$D_2(1,4) = (y_2 + y_3 - 2y_4)/12$$
$$D_2(1,5) = (4y_2 - y_3 - 3y_4)/72$$
$$D_2(1,6) = (3y_2 - y_3 - 2y_4)/72$$
$$D_2(1,7) = (2y_2 + y_3 - 3y_4)/72$$
$$D_2(1,8) = (3y_2 + y_3 - 4y_4)/72$$
$$D_2(1,9) = 0$$
$$D_2(1,10) = 0$$
$$D_2(1,11) = 0$$
$$D_2(1,12) = 0$$
$$D_2(1,13) = 0$$
$$D_2(1,14) = 0$$
$$D_2(1,15) = 0$$
$$D_2(1,16) = 0$$
$$D_2(2,1) = 0$$
$$D_2(2,2) = 0$$
$$D_2(2,3) = 0$$
$$D_2(2,4) = 0$$
$$D_2(2,5) = 0$$
$$D_2(2,6) = 0$$
$$D_2(2,7) = 0$$
$$D_2(2,8) = 0$$
$$D_2(2,9) = (-x_2 + x_4)/6$$
$$D_2(2,10) = (-2x_2 + x_3 + x_4)/12$$
$$D_2(2,11) = (-x_2 + x_4)/12$$
$$D_2(2,12) = (-x_2 - x_3 + 2x_4)/12$$
$$D_2(2,13) = (-4x_2 + x_3 + 3x_4)/72$$
$$D_2(2,14) = (-3x_2 + x_3 + 2x_4)/72$$
$$D_2(2,15) = (-2x_2 - x_3 + 3x_4)/72$$
$$D_2(2,16) = (-3x_2 - x_3 + 4x_4)/72$$
$$D_2(3,1) = (-2y_1 + y_3 + y_4)/12$$

$D_2(3,2) = (-y_1 + y_3)/6$

$D_2(3,3) = (-y_1 + 2y_3 - y_4)/12$

$D_2(3,4) = (-y_1 + y_3)/12$

$D_2(3,5) = (-4y_1 + 3y_3 + y_4)/72$

$D_2(3,6) = (-3y_1 + 4y_3 - y_4)/72$

$D_2(3,7) = (-2y_1 + 3y_3 - y_4)/72$

$D_2(3,8) = (-3y_1 + 2y_3 + y_4)/72$

$D_2(3,9)=0$

$D_2(3,10) = 0$

$D_2(3,11) = 0$

$D_2(3,12) = 0$

$D_2(3,13) = 0$

$D_2(3,14) = 0$

$D_2(3,15) = 0$

$D_2(3,16) = 0$

$D_2(4,1) = 0$

$D_2(4,2) = 0$

$D_2(4,3) = 0$

$D_2(4,4) = 0$

$D_2(4,5) = 0$

$D_2(4,6) = 0$

$D_2(4,7) = 0$

$D_2(4,8) = 0$

$D_2(4,9) = (2x_1 - x_3 - x_4)/12$

$D_2(4,10) = (x_1 - x_3)/6$

$D_2(4,11) = (x_1 - 2x_3 + x_4)/12$

$D_2(4,12) = (x_1 - x_3)/12$

$D_2(4,13) = (4x_1 - 3x_3 - x_4)/72$

$D_2(4,14) = (3x_1 - 4x_3 + x_4)/72$

$D_2(4,15) = (2x_1 - 3x_3 + x_4)/72$

$D_2(4,16) = (3x_1 - 2x_3 - x_4)/72$

$D_2(5,1) = (-y_2 + y_4)/12$

$D_2(5,2) = (y_1 - 2y_2 + y_4)/12$

$D_2(5,3) = (-y_2 + y_4)/6$

$D_2(5,4) = (-y_1 - y_2 + 2y_4)/12$

$D_2(5,5) = (y_1 - 3y_2 + 2y_4)/72$

$D_2(5,6) = (y_1 - 4y_2 + 3y_4)/72$

$D_2(5,7) = (-y_1 - 3y_2 + 4y_4)/72$

$D_2(5,8) = (-y_1 - 2y_2 + 3y_4)/72$

$D_2(5,9) = 0$

$D_2(5,10) = 0$

$D_2(5,11) = 0$

$D_2(5,12) = 0$

$D_2(5,13) = 0$

$D_2(5,14) = 0$

$D_2(5,15) = 0$

$D_2(5,16) = 0$

$D_2(6,1) = 0$

$D_2(6,2) = 0$

$D_2(6,3) = 0$

$D_2(6,4) = 0$

$D_2(6,5) = 0$

$D_2(6,6) = 0$

$D_2(6,7) = 0$

$D_2(6,8) = 0$

$D_2(6,9) = (x_2 - x_4)/12$

$D_2(6,10) = (-x_1 + 2x_2 - x_4)/12$

$D_2(6,11) = (x_2 - x_4)/6$

$D_2(6,12) = (x_1 + x_2 - 2x_4)/12$

$D_2(6,13) = (-x_1 + 3x_2 - 2x_4)/72$

$D_2(6,14) = (-x_1 + 4x_2 - 3x_4)/72$

$D_2(6,15) = (x_1 + 3x_2 - 4x_4)/72$

$D_2(6,16) = (x_1 + 2x_2 - 3x_4)/72$

$D_2(7,1) = (2y_1 - y_2 - y_3)/12$

$D_2(7,2) = (y_1 - y_3)/12$

$D_2(7,3) = (y_1 + y_2 - 2y_3)/12$

$D_2(7,4) = (y_1 - y_3)/6$

$D_2(7,5) = (3y_1 - y_2 - 2y_3)/72$

$D_2(7,6) = (2y_1 + y_2 - 3y_3)/72$

$D_2(7,7) = (3y_1 + y_2 - 4y_3)/72$

$D_2(7,8) = (4y_1 - y_2 - 3y_3)/72$

$D_2(7,9) = 0$

$D_2(7,10) = 0$

$D_2(7,11) = 0$

$D_2(7,12) = 0$

$D_2(7,13) = 0$

$D_2(7,14) = 0$

$D_2(7,15) = 0$

$D_2(7,16) = 0$

$D_2(8,1) = 0$

$D_2(8,2) = 0$

$D_2(8,3) = 0$

$D_2(8,4) = 0$

$D_2(8,5) = 0$

$D_2(8,6) = 0$

$D_2(8,7) = 0$

$D_2(8,8) = 0$

$D_2(8,9) = (-2x_1 + x_2 + x_3)/12$

$D_2(8,10) = (-x_1 + x_3)/12$

$D_2(8,11) = (-x_1 - x_2 + 2x_3)/12$

$D_2(8,12) = (-x_1 + x_3)/6$

$D_2(8,13) = (-3x_1 + x_2 + 2x_3)/72$

$D_2(8,14) = (-2x_1 - x_2 + 3x_3)/72$

$D_2(8,15) = (-3x_1 - x_2 + 4x_3)/72$

$D_2(8,16) = (-4x_1 + x_2 + 3x_3)/72$

$D_2(9,1) = (-6y_1 + 2y_2 + y_3 + 3y_4)/72$

$D_2(9,2) = (-2y_1 + 6y_2 - 3y_3 - y_4)/72$

$D_2(9,3) = (-y_1 + 3y_2 - 2y_4)/72$

$D_2(9,4) = (-3y_1 + y_2 + 2y_3)/72$

$D_2(9,5) = (-y_1 + y_2)/60$

$D_2(9,6) = (-y_1 + 3y_2 - y_3 - y_4)/144$

$D_2(9,7) = (-y_1 + y_2 + y_3 - y_4)/120$

$D_2(9,8) = (-3y_1 + y_2 + y_3 + y_4)/144$

$D_2(9,9) = 0$

$D_2(9,10) = 0$

$D_2(9,12) = 0$

$D_2(9,13) = 0$

$D_2(9,14) = 0$

$D_2(9,15) = 0$

$D_2(9,16) = 0$

$D_2(10,1) = 0$

$D_2(10,2) = 0$

$D_2(10,3) = 0$

$D_2(10,4) = 0$

$D_2(10,5) = 0$

$D_2(10,6) = 0$

$D_2(10,7) = 0$

$D_2(10,9) = (6x_1 - 2x_2 - x_3 - 3x_4)/72$

$D_2(10,10) = (2x_1 - 6x_2 + 3x_3 + x_4)/72$

$D_2(10,11) = (x_1 - 3x_2 + 2x_4)/72$

$D_2(10,12) = (3x_1 - x_2 - 2x_3)/72$

$D_2(10,13) = (x_1 - x_2)/60$

$D_2(10,14) = (x_1 - 3x_2 + x_3 + x_4)/144$

$D2(10,15) = (x_1 - x_2 - x_3 + x_4)/120$

$D_2(10,16) = (3x_1 - x_2 - x_3 - x_4)/144$

$D_2(11,1) = (-3y_2 + y_3 + 2y_4)/72$

$D_2(11,2) = (3y_1 - 6y_2 + 2y_3 + y_4)/72$

$D_2(11,3) = (-y_1 - 2y_2 + 6y_3 - 3y_4)/72$

$D_2(11,4) = (-2y_1 - y_2 + 3y_3)/72$

$D_2(11,5) = (y_1 - 3y_2 + y_3 + y_4)/144$

$D_2(11,6) = (-y_2 + y_3)/60$

$D_2(11,7) = (-y_1 - y_2 + 3y_3 - y_4)/144$

$D_2(11,8) = (-y_1 - y_2 + y_3 + y_4)/120$

$D_2(11,9) = 0$

$D_2(11,10) = 0$

$D_2(11,11) = 0$

$D_2(11,12) = 0$

$D_2(11,13) = 0$

$D_2(11,14) = 0$

$D_2(11,15) = 0$

$D_2(11,16) = 0$

$D_2(12,1) = 0$

$D_2(12,2) = 0$

$D_2(12,3) = 0$

$D_2(12,4) = 0$

$D_2(12,5) = 0$

$D_2(12,6) = 0$

$D_2(12,7) = 0$

$D_2(12,8) = 0$

$D_2(12,9) = (3x_2 - x_3 - 2x_4)/72$

$D_2(12,10) = (-3x_1 + 6x_2 - 2x_3 - x_4)/72$

$D_2(12,11) = (x_1 + 2x_2 - 6x_3 + 3x_4)/72$

$D_2(12,12) = (2x_1 + x_2 - 3x_3)/72$

$D_2(12,13) = (-x_1 + 3x_2 - x_3 - x_4)/144$

$D_2(12,14) = (x_2 - x_3)/60$

$D_2(12,15) = (x_1 + x_2 - 3x_3 + x_4)/144$

$D_2(12,16) = (x_1 + x_2 - x_3 - x_4)/120$

$D_2(13,1) = (-2y_2 - y_3 + 3y_4)/72$

$D_2(13,2) = (2y_1 - 3y_3 + y_4)/72$

$D_2(13,3) = (y_1 + 3y_2 - 6y_3 + 2y_4)/72$

$D_2(13,4) = (-3y_1 - y_2 - 2y_3 + 6y_4)/72$

$D_2(13,5) = (y_1 - y_2 - y_3 + y_4)/120$

$D_2(13,6) = (y_1 + y_2 - 3y_3 + y_4)/144$

$D_2(13,7) = (-y_3 + y_4)/60$

$D_2(13,8) = (-y_1 - y_2 - y_3 + 3y_4)/144$

$D_2(13,9) = 0$

$D_2(13,10) = 0$

$D_2(13,11) = 0$

$D_2(13,12) = 0$

$D_2(13,13) = 0$

$D_2(13,14) = 0$

$D_2(13,15) = 0$

$D_2(13,16) = 0$

$D_2(14,1) = 0$

$D_2(14,2) = 0$

$D_2(14,3) = 0$

$D_2(14,4) = 0$

$D_2(14,5) = 0$

$D_2(14,6) = 0$

$D_2(14,7) = 0$

$D_2(14,8) = 0$

$D_2(14,9) = (2x_2 + x_3 - 3x_4)/72$

$D_2(14,10) = (-2x_1 + 3x_3 - x_4)/72$

$D_2(14,11) = (-x_1 - 3x_2 + 6x_3 - 2x_4)/72$

$D_2(14,12) = (3x_1 + x_2 + 2x_3 - 6x_4)/72$

$D_2(14,13) = (-x_1 + x_2 + x_3 - x_4)/120$

$D_2(14,14) = (-x_1 - x_2 + 3x_3 - x_4)/144$

$D_2(14,15) = (x_3 - x_4)/60$

$D_2(14,16) = (x_1 + x_2 + x_3 - 3x_4)/144$

$D_2(15,1) = (6y_1 - 3y_2 - y_3 - 2y_4)/72$

$D_2(15,2) = (3y_1 - 2y_3 - y_4)/72$

$D_2(15,3) = (y_1 + 2y_2 - 3y_4)/72$

$D_2(15,4) = (2y_1 + y_2 + 3y_3 - 6y_4)/72$

$D_2(15,5) = (3y_1 - y_2 - y_3 - y_4)/144$

$D_2(15,6) = (y_1 + y_2 - y_3 - y_4)/120$

$D_2(15,7) = (y_1 + y_2 + y_3 - 3y_4)/144$

$D_2(15,8) = (y_1 - y_4)/60$

$D_2(15,9) = 0$

$D_2(15,10) = 0$

$D_2(15,11) = 0$

$D_2(15,12) = 0$

$D_2(15,13) = 0$

$D_2(15,14) = 0$

$D_2(15,15) = 0$

$D_2(15,16) = 0$

$D_2(16,1) = 0$

$D_2(16,2) = 0$

$D_2(16,3) = 0$

$D_2(16,4) = 0$

$D_2(16,5) = 0$

$D_2(16,6) = 0$

$D_2(16,7) = 0$

$D_2(16,8) = 0$

$D_2(16,9) = (-6x_1 + 3x_2 + x_3 + 2x_4)/72$

$D_2(16,10) = (-3x_1 + 2x_3 + x_4)/72$

$D_2(16,11) = (-x_1 - 2x_2 + 3x_4)/72$

$$D_2(16,12) = (-2x_1 - x_2 - 3x_3 + 6x_4)/72$$
$$D_2(16,13) = (-3x_1 + x_2 + x_3 + x_4)/144$$
$$D_2(16,14) = (-x_1 - x_2 + x_3 + x_4)/120$$
$$D_2(16,15) = (-x_1 - x_2 - x_3 + 3x_4)/144$$
$$D_2(16,16) = (-x_1 + x_4)/60 \qquad \text{(B.11)}$$

As with the thermal formulation, the boundary matrix [B] used in the structural formulation is evaluated over the element surface using the one-dimensional element interpolation functions. The coefficients in the structural boundary matrix are given by

$$B(1,1) = L/2$$
$$B(1,2) = 0$$
$$B(2,1) = 0$$
$$B(2,2) = L/2$$
$$B(3,1) = L/2$$
$$B(3,2) = 0$$
$$B(4,1) = 0$$
$$B(4,2) = L/2$$
$$B(5,1) = L/6$$
$$B(5,2) = 0$$
$$B(6,1) = 0$$
$$B(6,2) = L/6 \qquad \text{(B.12)}$$

where L is the length of the element edge where the applied pressure is defined. The mechanical stress component vector $\{ \overline{\sigma_1} \}$ is defined in equation (4.50) as $\{ \overline{\sigma_1} \} = [P]\{\delta\}$, where the coefficients in the matrix [P] are given by

$$P(1,1) = c_{11}(y_2 - y_4)/down1$$
$$P(1,2) = c_{12}(-x_2 + x_4)/down1$$
$$P(1,3) = c_{11}(-y_1 + y_4)/down1$$
$$P(1,4) = -c_{12}(-x_1 + x_4)/down1$$
$$P(1,5) = 0$$

$P(1,6) = 0$

$P(1,7) = -c_{11}(-y_1 + y_2)/down1$

$P(1,8) = c_{12}(-x_1 + x_2)/down1$

$P(1,9) = c_{11}(-y_1 + y_4)/down1$

$P(1,10) = -c_{12}(-x_1 + x_4)/down1$

$P(1,11) = 0$

$P(1,12) = 0$

$P(1,13) = 0$

$P(1,14) = 0$

$P(1,15) = -c_{11}(-y_1 + y_2)/down1$

$P(1,16) = c_{12}(-x_1 + x_2)/down1$

$P(2,1) = -c_{11}(-y_2 + y_3)/down2$

$P(2,2) = c_{12}(-x_2 + x_3)/down2$

$P(2,3) = c_{11}(-y_1 + y_3)/down2$

$P(2,4) = c_{12}(x_1 - x_3)/down2$

$P(2,5) = -c_{11}(-y_1 + y_2)/down2$

$P(2,6) = c_{12}(-x_1 + x_2)/down2$

$P(2,7) = 0$

$P(2,8) = 0$

$P(2,9) = -c_{11}(-y_2 + y_3)/down2$

$P(2,10) = c_{12}(-x_2 + x_3)/down2$

$P(2,11) = -c_{11}(-y_1 + y_2)/down2$

$P(2,12) = c_{12}(-x_1 + x_2)/down2$

$P(2,13) = 0$

$P(2,14) = 0$

$P(2,15) = 0$

$P(2,16) = 0$

$P(3,1) = 0$

$P(3,2) = 0$

$P(3,3) = c_{11}(y_3 - y_4)/down3$

$P(3,4) = -c_{12}(x_3 - x_4)/down3$

$P(3,5) = c_{11}(-y_2 + y_4)/down3$

$P(3,6) = c_{12}(x_2 - x_4)/down3$

$P(3,7) = -c_{11}(-y_2 + y_3)/down3$

$P(3,8) = c_{12}(-x_2 + x_3)/down3$

$P(3,9) = 0$

$P(3,10) = 0$

$P(3,11) = c_{11}(y_3 - y_4)/down3$

$P(3,12) = -c_{12}(x_3 - x_4)/down3$

$P(3,13) = -c_{11}(-y_2 + y_3)/down3$

$P(3,14) = c_{12}(-x_2 + x_3)/down3$

$P(3,15) = 0$

$P(3,16) = 0$

$P(4,1) = c_{11}(y_3 - y_4)/down4$

$P(4,2) = -c_{12}(x_3 - x_4)/down4$

$P(4,3) = 0$

$P(4,4) = 0$

$P(4,5) = c_{11}(-y_1 + y_4)/down4$

$P(4,6) = -c_{12}(-x_1 + x_4)/down4$

$P(4,7) = c_{11}(y_1 - y_3)/down4$

$P(4,8) = c_{12}(-x_1 + x_3)/down4$

$P(4,9) = 0$

$P(4,10) = 0$

$P(4,11) = 0$

$P(4,12) = 0$

$P(4,13) = c_{11}(-y_1 + y_4)/down4$

$P(4,14) = -c_{12}(-x_1 + x_4)/down4$

$P(4,15) = c_{11}(y_3 - y_4)/down4$

$P(4,16) = -c_{12}(x_3 - x_4)/down4$

$P(5,1) = c_{21}(y_2 - y_4)/down1$

$P(5,2) = c_{21}(-y_1 + y_4)/down1$

$P(5,4) = -c_{22}(-x_1 + x_4)/down1$

$P(5,5) = 0$

$P(5,6) = 0$

$P(5,7) = -c_{21}(-y_1 + y_2)/down1$

$P(5,8) = c_{22}(-x_1 + x_2)/down1$

$P(5,9) = c_{21}(-y_1 + y_4)/down1$

$P(5,10) = -c_{22}(-x_1 + x_4)/down1$

$P(5,11) = 0$

$P(5,12) = 0$

$P(5,13) = 0$

$P(5,14) = 0$

$P(5,15) = -c_{21}(-y_1 + y_2)/down1$

$P(5,16) = c_{22}(-x_1 + x_2)/down1$

$P(6,1) = -c_{21}(-y_2 + y_3)/down2$

$P(6,2) = c_{22}(-x_2 + x_3)/down2$

$P(6,3) = c_{21}(-y_1 + y_3)/down2$

$P(6,4) = c_{22}(x_1 - x_3)/down2$

$P(6,5) = -c_{21}(-y_1 + y_2)/down2$

$P(6,6) = c_{22}(-x_1 + x_2)/down2$

$P(6,7) = 0$

$P(6,8) = 0$

$P(6,9) = -c_{21}(-y_2 + y_3)/down2$

$P(6,10) = c_{22}(-x_2 + x_3)/down2$

$P(6,11) = -c_{21}(-y_1 + y_2)/down2$

$P(6,12) = c_{22}(-x_1 + x_2)/down2$

$P(6,13) = 0$

$P(6,14) = 0$

$P(6,15) = 0$

$P(6,16) = 0$

$P(7,1) = 0$

$P(7,2) = 0$

$P(7,4) = -c_{22}(x_3 - x_4)/down3$

$P(7,5) = c_{21}(-y_2 + y_4)/down3$

$P(7,6) = c_{22}(x_2 - x_4)/down3$

$P(7,7) = -c_{21}(-y_2 + y_3)/down3$

$P(7,8) = c_{22}(-x_2 + x_3)/down3$

$P(7,9) = 0$

$P(7,10) = 0$

$P(7,11) = c_{21}(y_3 - y_4)/down3$

$P(7,12) = -c_{22}(x_3 - x_4)/down3$

$P(7,13) = -c_{21}(-y_2 + y_3)/down3$

$P(7,14) = c_{22}(-x_2 + x_3)/down3$

$P(7,15) = 0$

$P(7,16) = 0$

$P(8,1) = c_{21}(y_3 - y_4)/down4$

$P(8,2) = -c_{22}(x_3 - x_4)/down4$

$P(8,3) = 0$

$P(8,4) = 0$

$P(8,5) = c_{21}(-y_1 + y_4)/down4$

$P(8,6) = -c_{22}(-x_1 + x_4)/down4$

$P(8,7) = c_{21}(y_1 - y_3)/down4$

$P(8,8) = c_{22}(-x_1 + x_3)/down4$

$P(8,9) = 0$

$P(8,10) = 0$

$P(8,11) = 0$

$P(8,12) = 0$

$P(8,13) = c_{21}(-y_1 + y_4)/down4$

$P(8,14) = -c_{22}(-x_1 + x_4)/down4$

$P(8,15) = c_{21}(y_3 - y_4)/down4$

$P(8,16) = -c_{22}(x_3 - x_4)/down4$

$P(9,1) = c_{33}(-x_2 + x_4)/down1$

$P(9,2) = c_{33}(y_2 - y_4)/down1$

$P(9,3) = -c_{33}(-x_1 + x_4)/down1$

$P(9,4) = c_{33}(-y_1 + y_4)/down1$

$P(9,5) = 0$

$P(9,6) = 0$

$P(9,7) = c_{33}(-x_1 + x_2)/down1$

$P(9,8) = -c_{33}(-y_1 + y_2)/down1$

$P(9,9) = -c_{33}(-x_1 + x4)/down1$

$P(9,10) = c_{33}(-y_1 + y_4)/down1$

$P(9,11) = 0$

$P(9,12) = 0$

$P(9,13) = 0$

$P(9,14) = 0$

$P(9,15) = c_{33}(-x_1 + x_2)/down1$

$P(9,16) = -c_{33}(-y_1 + y_2)/down1$

$P(10,1) = c_{33}(-x_2 + x_3)/down2$

$P(10,2) = -c_{33}(-y_2 + y_3)/down2$

$P(10,3) = c_{33}(x_1 - x_3)/down2$

$P(10,4) = c_{33}(-y_1 + y_3)/down2$

$P(10,5) = c_{33}(-x_1 + x_2)/down2$

$P(10,6) = -c_{33}(-y_1 + y_2)/down2$

$P(10,7) = 0$

$P(10, 8) = 0$

$P(10, 9) = c_{33}(-x_2 + x_3)/down2$

$P(10,10) = -c_{33}(-y_2 + y_3)/down2$

$P(10,11) = c_{33}(-x_1 + x_2)/down2$

$P(10,12) = -c_{33}(-y_1 + y_2)/down2$

$P(10,13) = 0$

$P(10,14) = 0$

$P(10,15) = 0$

$P(10,16) = 0$

$P(11, 1) = 0$

$P(11, 2) = 0$

$P(11, 3) = -c_{33}(x_3 - x_4)/down3$

$P(11, 4) = c_{33}(y_3 - y_4)/down3$

$P(11, 5) = c_{33}(x_2 - x_4)/down3$

$P(11, 6) = c_{33}(-y_2 + y_4)/down3$

$P(11, 7) = c_{33}(-x_2 + x_3)/down3$

$P(11, 8) = -c_{33}(-y_2 + y_3)/down3$

$P(11, 9) = 0$

$P(11,10) = 0$

$P(11,11) = -c_{33}(x_3 - x_4)/down3$

$P(11,12) = c_{33}(y_3 - y_4)/down3$

$P(11,13) = c_{33}(-x_2 + x_3)/down3$

$P(11,14) = -c_{33}(-y_2 + y_3)/down3$

$P(11,15) = 0$

$P(11,16) = 0$

$P(12, 1) = -c_{33}(x_3 - x_4)/down4$

$P(12, 2) = c_{33}(y_3 - y_4)/down4$

$P(12, 3) = 0$

$P(12, 4) = 0$

$P(12, 5) = -c_{33}(-x_1 + x_4)/down4$

$P(12, 6) = c_{33}(-y_1 + y_4)/down4$

$P(12, 7) = c_{33}(-x_1 + x_3)/down4$

$P(12, 8) = c_{33}(y_1 - y_3)/down4$

$P(12, 9) = 0$

$P(12,10) = 0$

$P(12,11) = 0$

$$
\begin{aligned}
P(12,12) &= 0 \\
P(12,13) &= -c_{33}(-x_1 + x_4)/down4 \\
P(12,14) &= c_{33}(-y_1 + y_4)/down4 \\
P(12,15) &= -c_{33}(x_3 - x_4)/down4 \\
P(12,16) &= c_{33}(y_3 - y_4)/down4
\end{aligned} \qquad \text{(B.13)}
$$

where down1, down2, down3, and down4 are defined by

$$
\begin{aligned}
down1 &= (x_2-x_1)y_4+(x_1-x_4)y_2+(x_4-x_2)y_1 \\
down2 &= (x_2-x_1)y_3+(x_1-x_3)y_2+(x_3-x_2)y_1 \\
down3 &= (x_3-x_2)y_4+(x_2-x_4)y_3+(x_4-x_3)y_2 \\
down4 &= (x_3-x_1)y_4+(x_1-x_4)y_3+(x_4-x_3)y_1
\end{aligned} \qquad \text{(B.14)}
$$

and c_{ij}, where i = 1 to 3 and j = 1 to 3, are the coefficients in the material elastic constant matrix defined in equation (4.40) for plane stress problems and equation (4.41) for plane strain problems. The coefficients in the thermal stress component vector $\overline{\{\sigma_2\}}$ are given by

$$
\begin{aligned}
\overline{\sigma_2}\,(1) &= \overline{\alpha}\,(c_{11} + c_{12})(T_1 - T_o) \\
\overline{\sigma_2}\,(2) &= \overline{\alpha}\,(c_{11} + c_{12})(T_2 - T_o) \\
\overline{\sigma_2}\,(3) &= \overline{\alpha}\,(c_{11} + c_{12})(T_3 - T_o) \\
\overline{\sigma_2}\,(4) &= \overline{\alpha}\,(c_{11} + c_{12})(T_4 - T_o) \\
\overline{\sigma_2}\,(5) &= \overline{\alpha}\,(c_{11} + c_{12})(T_5) \\
\overline{\sigma_2}\,(6) &= \overline{\alpha}\,(c_{11} + c_{12})(T_6) \\
\overline{\sigma_2}\,(7) &= \overline{\alpha}\,(c_{11} + c_{12})(T_7) \\
\overline{\sigma_2}\,(8) &= \overline{\alpha}\,(c_{11} + c_{12})(T_8) \\
\overline{\sigma_2}\,(9) &= \overline{\alpha}\,(c_{21} + c_{22})(T_1 - T_o) \\
\overline{\sigma_2}\,(10) &= \overline{\alpha}\,(c_{21} + c_{22})(T_2 - T_o) \\
\overline{\sigma_2}\,(11) &= \overline{\alpha}\,(c_{21} + c_{22})(T_3 - T_o)
\end{aligned}
$$

$$\overline{\sigma_2}\,(12) = \overline{\alpha}\,(c_{21} + c_{22})(T_4 - T_o)$$
$$\overline{\sigma_2}\,(13) = \overline{\alpha}\,(c_{21} + c_{22})(T_5)$$
$$\overline{\sigma_2}\,(14) = \overline{\alpha}\,(c_{21} + c_{22})(T_6)$$
$$\overline{\sigma_2}\,(15) = \overline{\alpha}\,(c_{21} + c_{22})(T_7)$$
$$\overline{\sigma_2}\,(16) = \overline{\alpha}\,(c_{21} + c_{22})(T_8) \qquad \text{(B.15)}$$

where cij, i = 1 to 3 and j = 1 to 3, are the coefficients in the material elastic constant matrix defined in equation (4.40) for plane stress problems and equation (4.41) for plane strain problems. For plane stress problems, $\overline{\alpha} = \alpha$ and for plane strain problems $\overline{\alpha} = \alpha(1+\nu)$.

REPORT DOCUMENTATION PAGE

Form Approved
OMB No. 0704-0188

1. AGENCY USE ONLY *(Leave blank)*	2. REPORT DATE	3. REPORT TYPE AND DATES COVERED
	April 1992	Technical Memorandum

4. TITLE AND SUBTITLE
Hierarchical Flux-Based Thermal-Structural Finite Element Analysis Method

5. FUNDING NUMBERS
WU 506-43-71-04

6. AUTHOR(S)
Sandra P. Polesky

7. PERFORMING ORGANIZATION NAME(S) AND ADDRESS(ES)
NASA Langley Research Center
Hampton, VA 23665-5225

8. PERFORMING ORGANIZATION REPORT NUMBER

9. SPONSORING / MONITORING AGENCY NAME(S) AND ADDRESS(ES)
National Aeronautics and Space Administration
Washington, DC 20546-0001

10. SPONSORING / MONITORING AGENCY REPORT NUMBER
NASA TM-107574

11. SUPPLEMENTARY NOTES

12a. DISTRIBUTION / AVAILABILITY STATEMENT
Unclassified - Unlimited

Subject Category - 39

12b. DISTRIBUTION CODE

13. ABSTRACT *(Maximum 200 words)*

A hierarchical flux-based finite element method is developed for both one- and two-dimensional thermal-structural analyses. Derivation of the finite element equations is presented. The resulting finite element matrices associated with the flux-based formulation are evaluated in closed-form. The hierarchical finite elements include additional degrees of freedom in the approximation of the element variable distributions by the use of nodeless variables. The nodeless variables offer increased solution accuracy without the need for defining actual nodes and rediscretizing the finite element model. Thermal and structural responses obtained from a conventional linear finite element method and exact solutions. Results show that the hierarchical flux-based method can provide improved thermal and structural solution accuracy with fewer elements when compared to results for the conventional linear element method.

14. SUBJECT TERMS	15. NUMBER OF PAGES
finite elements, hierarchical method, higher-order elements, flux-based formulation, thermal and structural analysis method	112
	16. PRICE CODE A06

17. SECURITY CLASSIFICATION OF REPORT	18. SECURITY CLASSIFICATION OF THIS PAGE	19. SECURITY CLASSIFICATION OF ABSTRACT	20. LIMITATION OF ABSTRACT
Unclassified	Unclassified	Unclassified	